DESIGN OF AN INERTIA MEASUREMENT DEVICE FOR STORES

A THESIS SUBMITTED TO
THE GRADUATE SCHOOL OF NATURAL AND APPLIED SCIENCES
OF
MIDDLE EAST TECHNICAL UNIVERSITY

BY

BERKAY KILIÇ

IN PARTIAL FULFILLMENT OF THE REQUIREMENTS
FOR
THE DEGREE OF MASTER OF SCIENCE
IN
MECHANICAL ENGINEERING

JUNE 2018

Approval of the thesis:

DESIGN OF AN INERTIA MEASUREMENT DEVICE FOR STORES

submitted by **BERKAY KILIÇ** in partial fulfillment of the requirements for the degree of **Master of Science in Mechanical Engineering Department, Middle East Technical University** by,

Prof. Dr. Halil Kalıpçılar
Dean, **Graduate School of Natural and Applied Sciences**   _____

Prof. Dr. M. A. Sahir Arıkan
Head of Department, **Mechanical Engineering**   _____

Asst. Prof. Dr. Hüsnü Dal
Supervisor, **Mechanical Engineering Dept., METU**   _____

Dr. Aydın Tüzün
Co-Supervisor, **TÜBİTAK SAGE**   _____

Examining Committee Members:

Prof. Dr. Serkan Dağ
Mechanical Engineering Dept., METU   _____

Asst. Prof. Dr. Hüsnü Dal
Mechanical Engineering Dept., METU   _____

Asst. Prof. Dr. Sezer Özerinç
Mechanical Engineering Dept., METU   _____

Asst. Prof. Dr. Batur Ercan
Metallurgical and Materials Engineering Dept., METU   _____

Assoc. Prof. Dr. Murat Demiral
Mechanical Engineering Dept., UTAA   _____

Date: 20.06.2018

I hereby declare that all information in this document has been obtained and presented in accordance with academic rules and ethical conduct. I also declare that, as required by these rules and conduct, I have fully cited and referenced all material and results that are not original to this work.

Name, Last Name :   Berkay KILIÇ

Signature   :

ABSTRACT

DESIGN OF AN INERTIA MEASUREMENT DEVICE FOR STORES

Kılıç, Berkay

M.Sc., Department of Mechanical Engineering

Supervisor   : Asst. Prof. Dr. Hüsnü Dal

Co-supervisor: Dr. Aydın Tüzün

June 2018, 99 pages

In this thesis, design of a device, which can measure mass properties of missiles or their sub-components in a single test setup, is expressed. An object, whose mass properties are going to be calculated, is attached to the device and three-dimensional, oscillatory motion about a specific point is supplied to that object. During this motion, velocity and acceleration values of the object are measured simultaneously with the force and torque values at the connection point. Mass properties of the object are computed by using measured velocity, acceleration, force and torque values in Newton's equations of motion.

Keywords: Mass Properties, Moments of Inertia, Products of Inertia

ÖZ

FÜZELERİN ATALET DEĞERLERİNİ ÖLÇEBİLECEK
BİR TEST SİSTEMİ TASARIMI

Kılıç, Berkay

Yüksek Lisans, Makina Mühendisliği Bölümü

Tez Yöneticisi   : Dr. Öğr. Üyesi Hüsnü Dal

Ortak Tez Yöneticisi: Dr. Aydın Tüzün

Haziran 2018, 99 sayfa

Bu tez çalışmasında, mühimmatların ve alt bileşenlerinin kütle özelliklerini, tek bir test kurulumu ile ölçebilen bir düzeneğin tasarımı anlatılmıştır. Kütle özellikleri ölçülmek istenen cisim, bu düzeneğe bağlanmakta ve cisme belirli bir nokta etrafında, üç boyutlu, salınımsal dönme hareketi verilmektedir. Bu hareket esnasında cismin hız ve ivme değerleri, cismin bağlantı noktasındaki kuvvet ve tork değerleri ile eşzamanlı olarak ölçülmektedir. Ölçülen hız, ivme, kuvvet ve tork değerleri, Newton'un hareket denklemlerinde kullanılarak cismin kütle özellikleri hesaplanmaktadır.

Anahtar Kelimeler: Kütle Özellikleri, Atalet Momentleri, Atalet Çarpımsalları

ACKNOWLEDGEMENTS

TABLE OF CONTENTS

LIST OF TABLES

TABLES

LIST OF FIGURES

FIGURES

CHAPTER 1

INTRODUCTION

1.1.   MASS PROPERTIES

In order to identify, monitor and control the motion of a body, its mass properties should be known. The mass properties of a rigid body are set of ten parameters consisting of a mass (m), center of gravity $(x_G, y_G$ and $z_G)$ and the inertia parameters $(I_{xx}, I_{yy}, I_{zz}, I_{xy}, I_{xz}, I_{yz})$.

Mass is a physical quantity which is the resistance of a body to change its linear acceleration when a force is applied to it. Mass of a solid body is defined by integral of density at each infinitesimal element of that body over the volume of the body as

$$m = \int_B \rho \, dV. \tag{1.1}$$
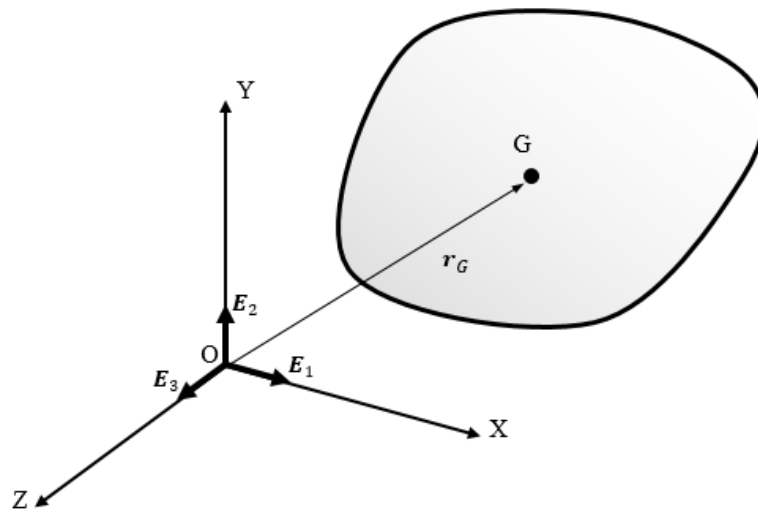
Figure 1. Center of gravity position of the given solid body is defined as
$$r_G = x_G \, E_1 + y_G \, E_2 + z_G \, E_3.$$

Center of gravity is a geometric property of a body. It is an imaginary point where the distribution of the mass of the body is balanced around as shown in Figure 1. If a force is applied to a body along its center of gravity point, it is going to move without rotating. In general, both the translational and rotational motion is described about the center of gravity point. Therefore, it is also convenient to describe inertia parameters about the center of gravity. Center of gravity can be defined relative to a reference point with the distances in any kind of a coordinate system.

Inertia is a tensor which is the resistance of a body to changes in its rotational motion when a torque is applied to it. In other words, it is a required torque for a desired angular acceleration about a rotational axis. Inertia parameters can be specified by the mass distribution of a body and the defined axes for inertia parameters. If a body is free to rotate about all three axes, its moment of inertia parameters can be described by a symmetric 3×3 matrix

$$
\boldsymbol{I} = \begin{bmatrix} I_{xx} & -I_{xy} & -I_{xz} \\ -I_{xy} & I_{yy} & -I_{yz} \\ -I_{xz} & -I_{yz} & I_{zz} \end{bmatrix}. \tag{1.2}
$$

The diagonal elements of the inertia tensor are the moment of inertia (MOI) parameters, and the non-diagonal elements of the inertia tensor are the product of inertia (POI) parameters.

Moment of inertia of a body about an axis is the measure of the distribution of the mass about that axis. If the axis is chosen close to the center of gravity, moment of inertia value about that axis is going to be smaller relative to an axis away from the center of gravity. For instance, I_{xx} is said to be the moment of inertia about x axis, and it can also be denoted as I_x.
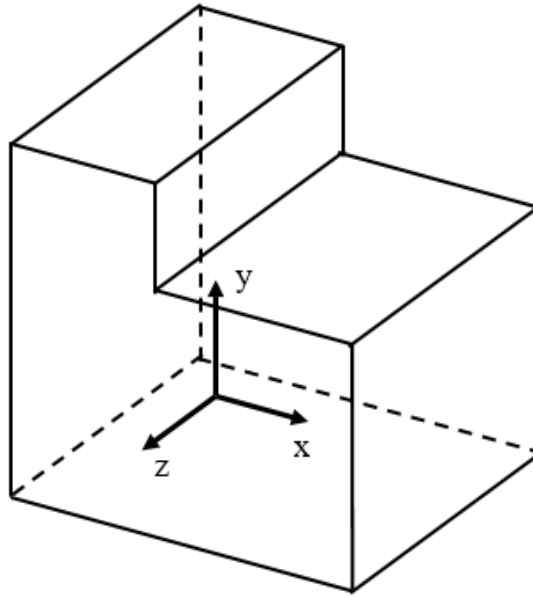
Figure 2. Solid body, whose symmetry plane is xy plane, is demonstrated.

Product of inertia of a body is the measure of symmetry relative to a plane. For instance, if xy plane is the plane of symmetry for a body as shown in Figure 2, product of inertias about the axis perpendicular to that plane (z axis) is going to be zero, $I_{xz} = I_{yz} = 0$.

For a point mass, inertia about an axis is the multiplication of mass and square of perpendicular distance to that axis. Inertia of a body can be calculated using the same sense with an integration over the body.

1.2.   OBJECTIVE AND MOTIVATION

In many engineering applications, such as design of a ground or an air vehicle, knowing the mass properties of a body plays a crucial role for rigid body dynamics. The structural design, motion control algorithms or computer simulations of a vehicle is based on the mass properties of it. Therefore, mass properties of the body in consideration should be measured properly.

For missiles also, measurement of mass properties is important in order to control and guide it. The mass parameters can be measured by using Computer Aided Design (CAD) tools. However, in reality, measurements of CAD tools vary from the real value

to some degree depending on the complexity of the assembly. Geometric tolerances, defects and non-homogeneous density of the components may cause that difference. Also, in some assemblies, some components are taken from third parties and integrated into the structure. Mass properties of these components are mostly unknown. Because of these, designing a system depending only on the mass properties measurement from the computer is not possible. Therefore, the most reliable method to get the mass properties of a body is to make an experimental measurement.

In the literature, there are wide range of studies to measure the mass properties experimentally. Some of these studies measure the mass properties through a set of tests, i.e., with the requirement of reassembling the test specimen more than one time. In such studies, making more than one test slows down the measurement procedure and increases the need for labor. Also, reassembling the specimen creates additional uncertainties to the results. Apart from these, there are some designs measuring the mass properties by a single test. These setups are more advantageous in terms of the speed and ease of the test configuration.

In this thesis, a test device is developed to measure mass properties of some systems, particularly subsystems of the missiles and missiles up to 20 kg. That test device is able to measure the complete mass properties in a single test. At the design stage of the test device, favorable and unfavorable aspects of the test setups in the literature are utilized and a new design is obtained.

1.3.   SCOPE OF THE THESIS

This thesis consists of five chapters. General information about the mass properties and the purpose of the thesis is given in Chapter 1. In Chapter 2, theoretical background is given to measure the mass properties along with the detailed information about the studies in the literature. In Chapter 3, working principles and the methodology to measurement procedure of the developed test device are explained. In Chapter 4, three different tests are performed and their results are compared with the theoretical values. Lastly in Chapter 5, conclusion of the study is given and the possible future works are suggested.

CHAPTER 2

THEORY AND LITERATURE

2.1. THEORETICAL BACKGROUND

In order to calculate the mass properties of a body, its equations of motion should be derived primarily. Deriving equations of motion of a body requires understanding of kinematics and kinetics of the body. Kinematics is the study of the motion of objects, that may be particles or bodies. It is described by positions, velocities and accelerations of objects without referring the forces acting on them. Besides that, kinetics is the analyses of forces, that causes motion, acting on objects. Kinetics also deals with the mass properties of the objects in addition to forces and torques acting on these objects.

It can be expressible that the rigid bodies comprise of particles. Particles have masses but they are treated as a point. Therefore, they can only have a translational motion. Their rotational motion is impractical. The inertia parameters are related to rotational motion, though particles do not have these mass parameters. They have only mass and location of gravity center parameters. In order to describe the motion of a rigid body; however, kinematics and kinetics of a particle should be a priori known. Then, kinematics and kinetics of a rigid body can be derived and equations of motion of a rigid body can be obtained. [1], [2] have been utilized and summarized through Chapter 2 in order to obtain equations of motion of a rigid body.

2.1.1. Kinematics of a Particle

Kinematics of a particle can be defined by position, velocity and acceleration of that particle. These kinematical quantities are described with respect to a coordinate system like shown in Figure 3.
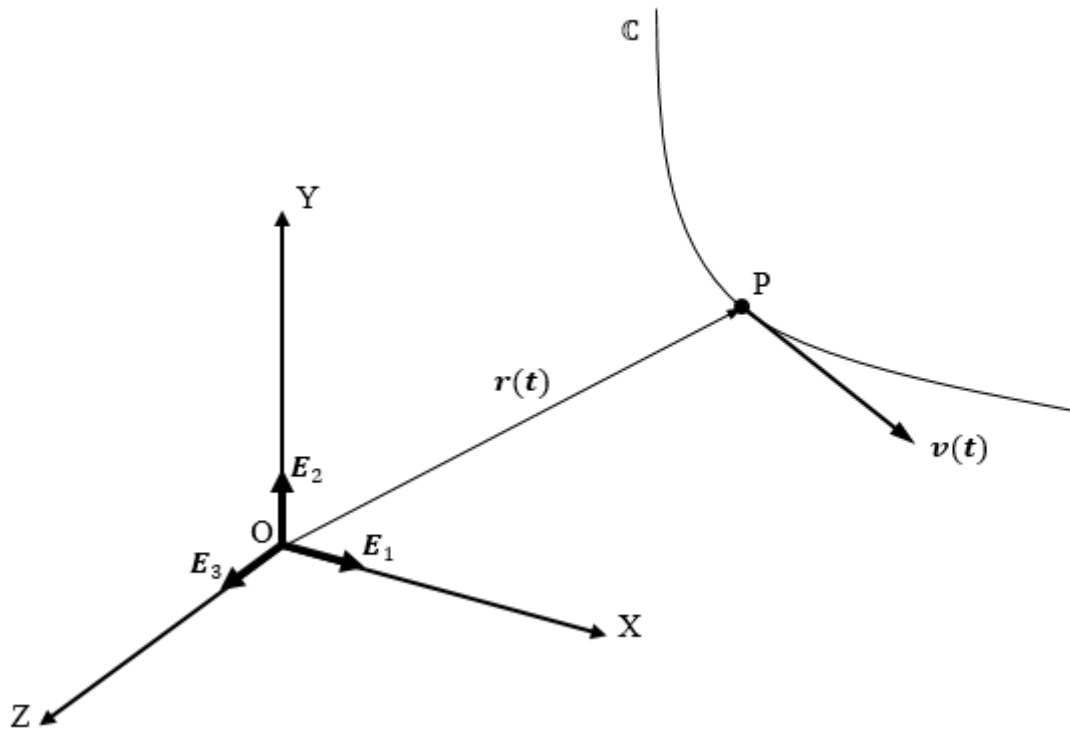
Figure 3. Particle P is moving along the shown path $\mathbb{C}$ with velocity $\boldsymbol{v}(t)$. Its position is described by the position vector $\boldsymbol{r}(t)$ at time t.

Position is the spatial location of the particle and described in 3-D Cartesian coordinate system as follows

$$\boldsymbol{r}(t) = r_x(t)\, \boldsymbol{E}_1 + r_y(t)\, \boldsymbol{E}_2 + r_z(t)\, \boldsymbol{E}_3. \tag{2.1}$$

Velocity is the rate of change of the position of the particle and described as

$$\boldsymbol{v} = \dot{\boldsymbol{r}} = \dot{r}_x\, \boldsymbol{E}_1 + \dot{r}_y\, \boldsymbol{E}_2 + \dot{r}_z\, \boldsymbol{E}_3. \tag{2.2}$$

Acceleration is the rate of change of the velocity of the particle and described as

$$\boldsymbol{a} = \dot{\boldsymbol{v}} = \ddot{\boldsymbol{r}} = \ddot{r}_x\, \boldsymbol{E}_1 + \ddot{r}_y\, \boldsymbol{E}_2 + \ddot{r}_z\, \boldsymbol{E}_3. \tag{2.3}$$

2.1.2. Kinetics of a Particle

Since kinetics is related to forces that causes motion, it starts with *Newton's second law of motion*. It is also known as *equations of motion* and can be formulated as

6

$$F = m\,a = m\,\dot{v} = m\,\frac{dv}{dt}, \qquad (2.4)$$

where m is the particle's mass, F is the force acting on the particle, a is the acceleration of the particle in Figure 4. If this equation of motion is integrated with respect to time, impulse and momentum relation can be obtained. Assuming that the particle has a velocity of v_1 at time t_1 and v_2 at time t_2, principle of impulse and momentum equation is written as

$$\int_{t_1}^{t_2} F\,dt = m\int_{v_1}^{v_2} dv, \qquad \int_{t_1}^{t_2} F\,dt = m\,(v_2 - v_1). \qquad (2.5)$$

Left hand side of equation is the linear impulse, which indicates the effect of a force acting on a particle over a specified time interval. The terms on the right side are linear momentums of the particle at time t_1 and t_2. Linear momentum of a particle can be defined as

$$L = m\,v. \qquad (2.6)$$

Therefore, force acting on a particle and linear impulse of that particle can be interrelated as

$$\sum F = \dot{L}. \qquad (2.7)$$

This equation states that the time rate of change of linear momentum is equals to the total force acting on a particle.

When a particle has linear momentum, it can be mentioned that the particle has also angular momentum about a point. Angular momentum is defined as the moment of the particle's linear momentum about a point. Therefore, angular momentum is also called as "moment of momentum".
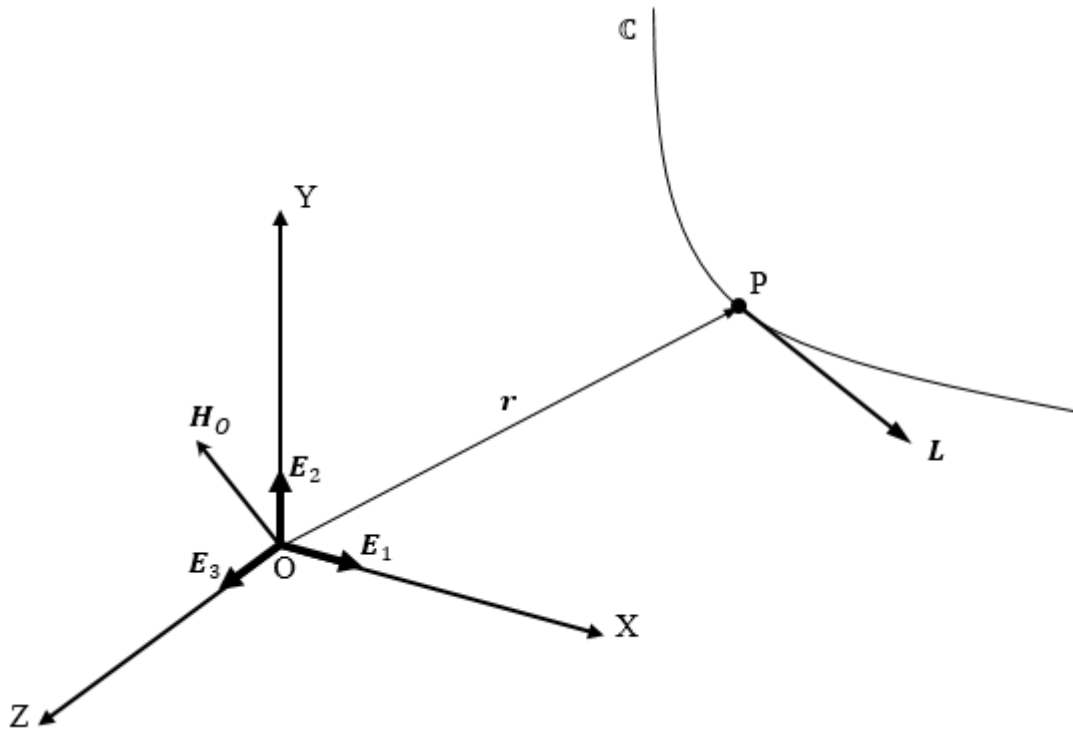
Figure 4. Representation of linear momentum $\boldsymbol{L}$ of particle P and resulted angular momentum $\boldsymbol{H}_o$ at point O.

Angular momentum is formulated by a cross product of the position vector with linear momentum vector

$$\boldsymbol{H}_O = \boldsymbol{r} \times \boldsymbol{L}. \tag{2.8}$$

Angular momentum definition is used to obtain a new form of the equation of motion. Differentiating the angular momentum definition with respect to time leads to create a relation between moment and angular momentum

$$\dot{\boldsymbol{H}}_O = \frac{d(\boldsymbol{r} \times \boldsymbol{L})}{dt} = \frac{d(\boldsymbol{r} \times m\,\boldsymbol{v})}{dt} = \dot{\boldsymbol{r}} \times m\,\boldsymbol{v} + \boldsymbol{r} \times m\,\dot{\boldsymbol{v}}. \tag{2.9}$$

Since $\dot{\boldsymbol{r}} \times m\,\boldsymbol{v} = \dot{\boldsymbol{r}} \times m\,\dot{\boldsymbol{r}} = m(\dot{\boldsymbol{r}} \times \dot{\boldsymbol{r}}) = \boldsymbol{0}$, the derivative of angular momentum definition becomes

$$\dot{\boldsymbol{H}}_O = \boldsymbol{r} \times m\,\dot{\boldsymbol{v}}. \tag{2.10}$$

8

The second term on the right hand side of the equation (2.10) is the force acting on the particle, and since $\boldsymbol{r} \times \boldsymbol{F}$ is the definition of moment, the equation (2.10) is also written as follows

$$\sum \boldsymbol{M} = \dot{\boldsymbol{H}}_O. \tag{2.11}$$

The equation (2.11) states that the time rate of change of particle's angular momentum about point O equals to the total moment on the particle about the same point O. This expression is analogous with the equation (2.7).

2.1.3. System of Particles

For the system of particles which is enclosed by dashed line as shown in Figure 5, linear impulse and linear momentum relation is obtained by using Newton's second law

$$\sum_{i=1}^{n} \boldsymbol{F}_i = \sum_{i=1}^{n} m_i \frac{d\boldsymbol{v}_i}{dt}. \tag{2.12}$$
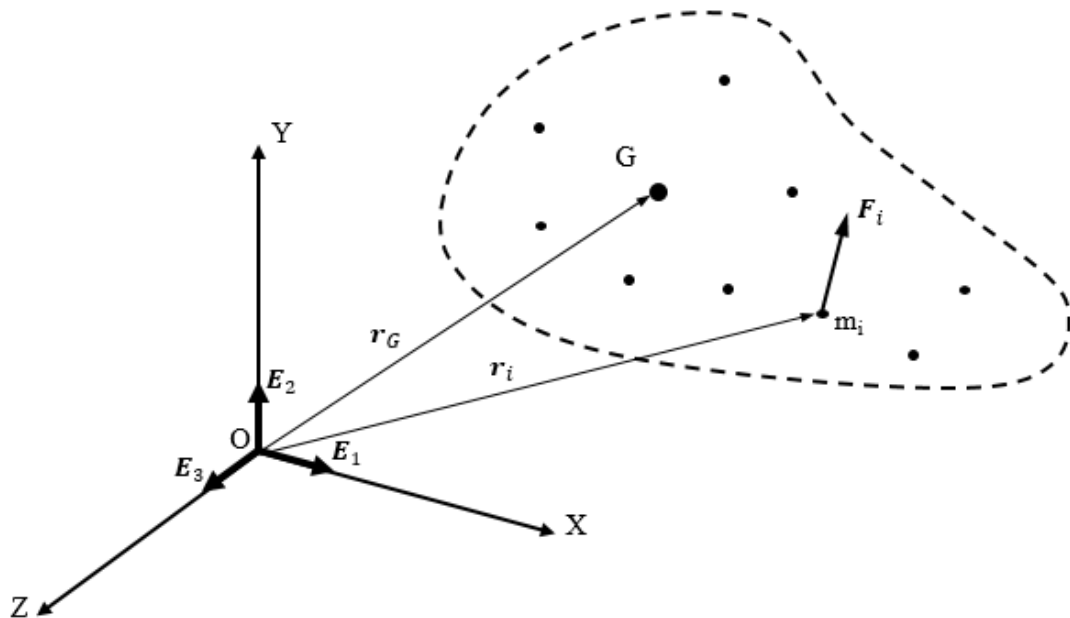
Figure 5. System of particles whose center of mass is located at G and force acting on one particle are demonstrated.

Principle of impulse and momentum for the system of particles is derived by integrating the equation (2.12) with a similar operation for one particle

$$\sum_{i=1}^{n} \int_{t_1}^{t_2} \boldsymbol{F}_i \, dt = \sum_{i=1}^{n} m_i \boldsymbol{v}_{i_2} - \sum_{i=1}^{n} m_i \boldsymbol{v}_{i_1}. \tag{2.13}$$

If it is assumed that the summation of the all particles' masses are $m = \Sigma \, m_i$, and center of mass of all particles are located at point G, total linear momentum of this system of particles is written as

$$\boldsymbol{L}_{total} = m \, \boldsymbol{v}_G = \sum_{i=1}^{n} m_i \boldsymbol{v}_i. \tag{2.14}$$

Similarly, an expression for the total moment acting on this system of particles may be derived using the summation of time rate of change of angular momentum for each individual particle

$$\sum_{i=1}^{n} \boldsymbol{M}_{O_i} = \sum_{i=1}^{n} \dot{\boldsymbol{H}}_{O_i} = \sum_{i=1}^{n} \boldsymbol{r}_i \times m_i \, \dot{\boldsymbol{v}}_i = \sum_{i=1}^{n} \boldsymbol{r}_i \times \boldsymbol{F}_i, \tag{2.15}$$

which may also be written as

$$\sum \boldsymbol{M}_O = \boldsymbol{r}_G \times m \, \dot{\boldsymbol{v}}_G. \tag{2.16}$$

Rigid bodies may be assumed as they are collection of infinitesimal particles that are fixed to each other. Therefore, equations (2.14) and (2.16) may be extended for rigid bodies and these finite summations are replaced with continuous equations as

$$\sum_{i=1}^{n} \boldsymbol{F}_i = \int_{\mathcal{B}} \boldsymbol{F}(t) \, dt,$$

$$\sum_{i=1}^{n} \boldsymbol{M}_{O_i} = \int_{\mathcal{B}} \boldsymbol{M}_O(t) \, dt. \tag{2.17}$$

Then, equations (2.17) are used to obtain general equations of motion for rigid bodies. Through these equations, mass parameters of rigid bodies are going to be calculated.

2.1.4. Kinematics of a Rigid Body

Motion of a rigid body may be in three different manners which are translation, rotation and combination of translation and rotation.

In *translational motion*, the rigid body does not change its orientation in space. Position vectors of any point on the rigid body changes with respect to a fixed point, but a vector which is drawn from one point to another point on the rigid body remains constant. The rigid body has translational velocity and acceleration similar to the particle's motion.

In *rotational motion*, the rigid body has an angular motion about a fixed point. All points on the rigid body move along circular paths. The position vector of any point changes its direction; however, its magnitude stays constant. In the concept of the rotational motion, angular position, angular velocity and angular acceleration are defined which are not exist in particle's motion.
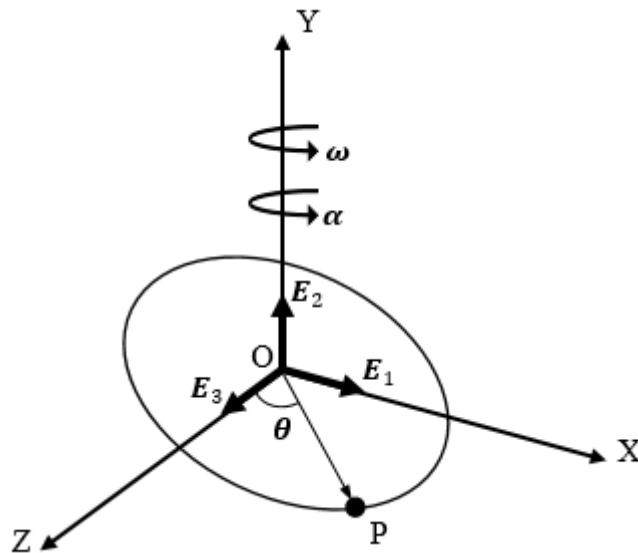
Figure 6. Particle P is moving along circular path. Its angular position $\boldsymbol{\theta}$, velocity $\boldsymbol{\omega}$, and acceleration $\boldsymbol{\alpha}$ about rotation axis is shown.

For point P in Figure 6, angular position is defined by an angle between a fixed reference and position vector of the point P

$$\boldsymbol{\theta} = \theta_x \, \boldsymbol{E}_1 + \theta_y \, \boldsymbol{E}_2 + \theta_z \, \boldsymbol{E}_3. \tag{2.18}$$

Angular velocity is the rate of change of the angular position and defined as follows

$$\boldsymbol{\omega} = \dot{\boldsymbol{\theta}} = \omega_x \, \boldsymbol{E}_1 + \omega_y \, \boldsymbol{E}_2 + \omega_z \, \boldsymbol{E}_3. \tag{2.19}$$

The direction of angular velocity, $\boldsymbol{\omega}$, is called as the instantaneous axis of rotation.

Angular acceleration is the rate of change of the angular velocity and defined as follows

$$\boldsymbol{\alpha} = \dot{\boldsymbol{\omega}} = \ddot{\boldsymbol{\theta}} = \alpha_x \, \boldsymbol{E}_1 + \alpha_y \, \boldsymbol{E}_2 + \alpha_z \, \boldsymbol{E}_3. \tag{2.20}$$

Translational velocity and acceleration of point P may be defined if the angular velocity, $\boldsymbol{\omega}$, and angular acceleration, $\boldsymbol{\alpha}$, are known at specific time as follows

$$\boldsymbol{v} = \frac{d\boldsymbol{r}}{dt} = \boldsymbol{\omega} \times \boldsymbol{r},$$

$$\boldsymbol{a} = \frac{d\boldsymbol{v}}{dt} = \frac{d\boldsymbol{\omega}}{dt} \times \boldsymbol{r} + \boldsymbol{\omega} \times \frac{d\boldsymbol{r}}{dt} = \boldsymbol{\alpha} \times \boldsymbol{r} + \boldsymbol{\omega} \times (\boldsymbol{\omega} \times \boldsymbol{r}). \tag{2.21}$$
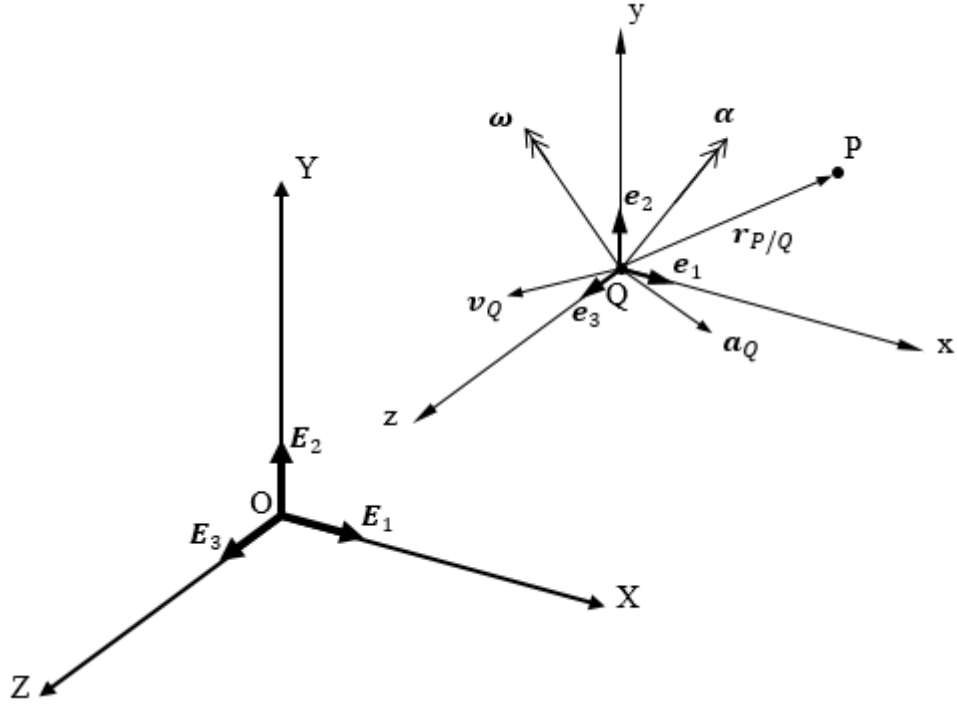
Figure 7. Position of point P with respect to translating and rotating coordinate system located at point Q. Translational and rotational motion of this local frame is defined relative to fixed reference coordinate system at point O.

The combination of translational and rotational motion is defined as *general motion*. If a rigid body has both translational and rotational motions and if its translational velocity v, translational acceleration a, angular velocity ω and angular acceleration α are known; velocity and acceleration of point P in Figure 7 may be defined as follows

$$v_P = v_Q + \omega \times r_{P/Q},$$

$$a_P = a_Q + \alpha \times r_{P/Q} + \omega \times (\omega \times r_{P/Q}).$$

(2.22)

In order to define the motion of a rigid body in the most general way, the equations (2.22) should be written by using a translating and rotating coordinate system (local frame, (xyz)) with respect to a fixed reference coordinate system (global frame, (XYZ)). In Figure 8, global frame is fixed and located at point O, while the local frame, which is attached to the rigid body at point Q, has both translational and rotational motion. It translates with velocity v_Q and acceleration a_Q with respect to

global frame. At the same time, it rotates with angular velocity, $\boldsymbol{\Omega}$, and angular acceleration, $\dot{\boldsymbol{\Omega}}$, with respect to global frame. Point P is an arbitrary point on the rigid body.
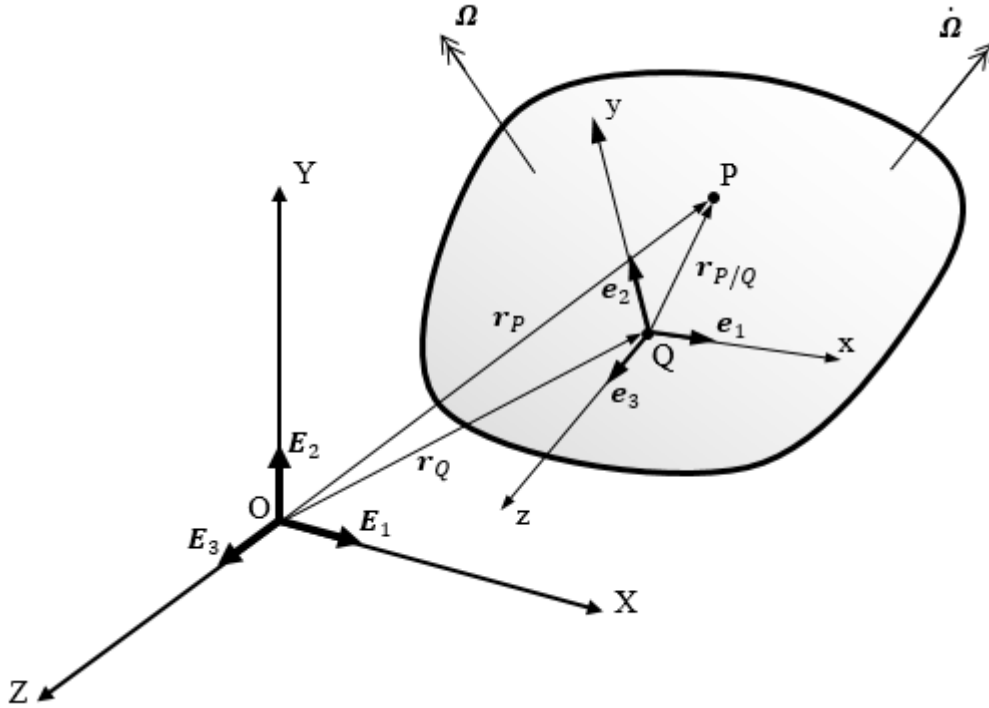
Figure 8. Local frame is located on a body which is in general motion. Kinematic of point P on the body is going to be analyzed.

The position vector of point P in global frame is defined as

$$\boldsymbol{r}_P = \boldsymbol{r}_Q + \boldsymbol{r}_{P/Q}, \tag{2.23}$$

where $\boldsymbol{r}_{P/Q}$ is the relative position vector of P with respect to Q.

The velocity vector of point P in global frame may be found by taking derivative of equation (2.23)

$$\dot{\boldsymbol{r}}_P = \dot{\boldsymbol{r}}_Q + \dot{\boldsymbol{r}}_{P/Q} \qquad \rightarrow \qquad \boldsymbol{v}_P = \boldsymbol{v}_Q + \dot{\boldsymbol{r}}_{P/Q}. \tag{2.24}$$

To calculate the derivative of $\boldsymbol{r}_{P/Q}$, it should be expressed in terms of its components in local frame as

$$r_{P/Q} = x_P\, e_1 + y_P\, e_2 + z_P\, e_3. \tag{2.25}$$

Taking derivative of equation (2.25) with respect to global frame gives

$$\dot{r}_{P/Q} = \dot{x}_P\, e_1 + \dot{y}_P\, e_2 + \dot{z}_P\, e_3 + x_P\, \dot{e}_1 + y_P\, \dot{e}_2 + z_P\, \dot{e}_3. \tag{2.26}$$

Time derivative of unit vectors of local frame with respect to global frame is calculated by using the angular velocity of local frame, $\boldsymbol{\Omega}$, as given in [1]

$$\dot{e}_1 = \boldsymbol{\Omega} \times e_1, \quad \dot{e}_2 = \boldsymbol{\Omega} \times e_2, \quad \dot{e}_3 = \boldsymbol{\Omega} \times e_3. \tag{2.27}$$

The first three terms of equation (2.26) is simply the derivative of $r_{P/Q}$ with respect to local frame. Therefore, $\dot{r}_{P/Q}$ vector is defined as follows

$$\dot{r}_{P/Q} = (\dot{r}_{P/Q})_{xyz} + \boldsymbol{\Omega} \times r_{P/Q},$$
$$v_{P/Q} = (v_{P/Q})_{xyz} + \boldsymbol{\Omega} \times r_{P/Q}. \tag{2.28}$$

Using equation (2.28), velocity vector of point P with respect to global frame is written as

$$v_P = v_Q + v_{P/Q} + \boldsymbol{\Omega} \times r_{P/Q}. \tag{2.29}$$

where $v_{P/Q}$ is the velocity of point P with respect to local frame.

Similarly, acceleration vector of point P with respect to global frame may be found by taking derivative of v_P

$$a_P = \dot{v}_P = \dot{v}_Q + \dot{v}_{P/Q} + \dot{\boldsymbol{\Omega}} \times r_{P/Q} + \boldsymbol{\Omega} \times \dot{r}_{P/Q}, \tag{2.30}$$

and when necessary operations are made, the following equation can be obtained

$$a_P = a_Q + (a_{P/Q})_{xyz} + \dot{\boldsymbol{\Omega}} \times r_{P/Q} + \boldsymbol{\Omega} \times (\boldsymbol{\Omega} \times r_{P/Q})$$
$$+ 2\,\boldsymbol{\Omega} \times (v_{P/Q})_{xyz}, \tag{2.31}$$

where $a_{P/Q}$ is the acceleration vector of point P with respect to local frame.

For the body shown in Figure 8, position vector of point P in the local frame, $r_{P/Q}$, is constant since the body is assumed as a rigid. Therefore, velocity and acceleration vectors of point P in the local frame, $v_{P/Q}$ and $a_{P/Q}$, disappear from the equations (2.29) and (2.31). Using that simplification, kinematic equations for a rigid body with respect to global frame is written as follows

$$r_P = r_Q + r_{P/Q},$$
$$v_P = v_Q + \boldsymbol{\Omega} \times r_{P/Q},$$
$$a_P = a_Q + \dot{\boldsymbol{\Omega}} \times r_{P/Q} + \boldsymbol{\Omega} \times (\boldsymbol{\Omega} \times r_{P/Q}).$$

(2.32)

2.1.5. Kinetics of a Rigid Body

In the equation (2.14), linear momentum is defined as the total mass of all particles times the velocity of center of gravity. This is also valid for a rigid body.

$$L = m\, v.$$

(2.33)
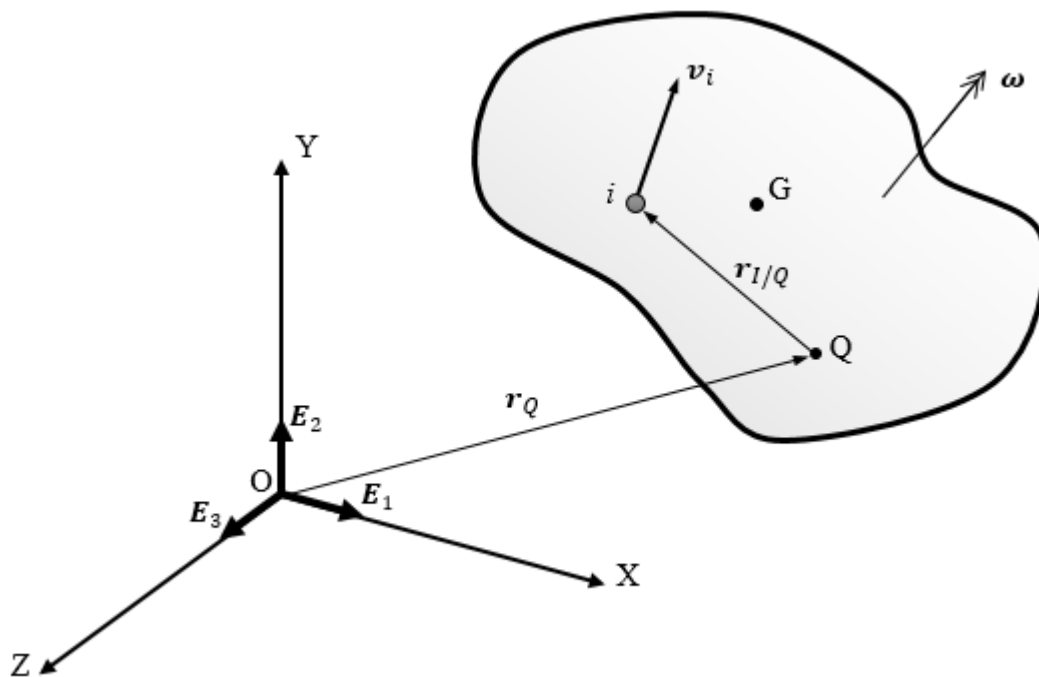
Figure 9. Kinetics of a rigid body is examined by using its particles' linear and angular momentums.

For a particle in the rigid body shown in Figure 9, angular momentum equation about point Q is written as follows

$$H_{Q_i} = r_{I/Q} \times m_i \, v_i. \tag{2.34}$$

If $v_i = v_Q + \omega \times r_Q$ is placed into equation (2.34),

$$\begin{aligned} H_{Q_i} &= r_{I/Q} \times m_i \left(v_Q + \omega \times r_Q \right) \\ &= r_{I/Q} \times m_i \, v_Q + r_{I/Q} \times m_i (\omega \times r_{I/Q}). \end{aligned} \tag{2.35}$$

If the equation (2.35) is integrated over the body, angular momentum of the body about the point Q is obtained as

$$H_Q = (\int r_{I/Q} \, dm) \times v_Q + \int r_{I/Q} \times (\omega \times r_{I/Q}) \, dm. \tag{2.36}$$

Expanding equation (2.36) in its Cartesian components will help to get the relation between the angular momentum and the inertia parameters

$$\begin{aligned} H_{Qx} \, e_1 &+ H_{Qy} \, e_2 + H_{Qz} \, e_3 \\ &= \int (x \, e_1 + y \, e_2 + z \, e_3) \times \left(v_{Qx} \, e_1 + v_{Qy} e_2 + v_{Qz} \, e_3 \right) dm \\ &+ \int \{ (x \, e_1 + y \, e_2 + z \, e_3) \times \left(\omega_x \, e_1 + \omega_y \, e_2 + \omega_z \, e_3 \right) \\ &\times (x \, e_1 + y \, e_2 + z \, e_3) \} dm. \end{aligned}$$

$$(2.37)$$

Taking the integral over the body and making the cross product operations yield

$$\begin{aligned} H_{Qx} \, e_1 &+ H_{Qy} \, e_2 + H_{Qz} \, e_3 \\ &= m \left[(y \, v_{Qz} - z \, v_{Qy}) \, e_1 + (z \, v_{Qx} - x \, v_{Qz}) \, e_2 + (x \, v - y \, v_{Qx}) \, e_3 \right] \\ &+ \left[\omega_x \int (y^2 + z^2) \, dm - \omega_y \int xy \, dm - \omega_z \int xz \, dm \right] e_1 \\ &+ \left[-\omega_x \int xy \, dm + \omega_y \int (x^2 + z^2) \, dm - \omega_z \int yz \, dm \right] e_2 \\ &+ \left[-\omega_x \int xz \, dm - \omega_y \int yz \, dm + \omega_z \int (x^2 + y^2) \, dm \right] e_3. \end{aligned}$$

17

2.1.6. Moments and Products of Inertia
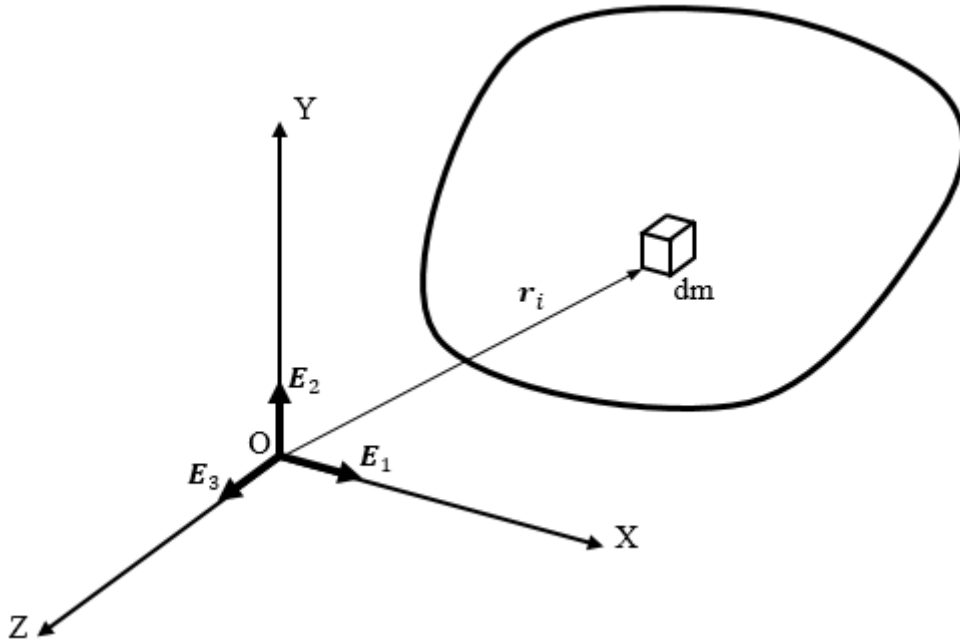
Figure 10. Differential element of mass dm relative to reference coordinate frame is shown.

For the differential element shown in Figure 10, moments of inertia about an axis can be defined as mass of the element multiplied by the shortest distance between the element and the corresponding axis. Therefore, if the moment of inertia of the differential element is integrated over the body, the following moment of inertia expressions can be obtained

$$I_{xx} = \int (y^2 + z^2)\, dm,$$

$$I_{yy} = \int (x^2 + z^2)\, dm, \qquad\qquad (2.39)$$

$$I_{zz} = \int (x^2 + y^2)\, dm.$$

Likewise, product of inertia of the differential element relative to two orthogonal planes can be defined as mass multiplied by the shortest distance between the element

and the corresponding planes. Therefore, if the product of inertia of the differential element is integrated over the body, the following product of inertia expressions can be obtained

$$I_{xy} = I_{yz} = \int xy \, dm,$$

$$I_{xz} = I_{zx} = \int xz \, dm, \qquad (2.40)$$

$$I_{yz} = I_{zy} = \int yz \, dm.$$

Moments and products of inertia definitions form the inertia tensor in the following form

$$\mathbf{I} = \begin{bmatrix} I_{xx} & -I_{xy} & -I_{xz} \\ -I_{xy} & I_{yy} & -I_{yz} \\ -I_{xz} & -I_{yz} & I_{zz} \end{bmatrix}. \qquad (2.41)$$

These moments and products of inertia definitions can be observed in the angular momentum expression in equation (2.38). Replacing these parameters into equation (2.38) gives the components of the angular momentum as follows

$$\begin{aligned} H_{Qx} &= m\left(y\, v_{Qz} - z\, v_{Qy}\right) + I_{xx}\, \omega_x - I_{xy}\, \omega_y - I_{xz}\, \omega_z, \\ H_{Qy} &= m\left(z\, v_{Qx} - x\, v_{Qz}\right) - I_{xy}\, \omega_x + I_{yy}\, \omega_y - I_{yz}\, \omega_z, \qquad (2.42) \\ H_{Qz} &= m\left(x\, v_{Qy} - y\, v_{Qx}\right) - I_{xz}\, \omega_x - I_{yz}\, \omega_y + I_{zz}\, \omega_z. \end{aligned}$$

2.1.7. Equations of Motion

Since a rigid body may be assumed to be comprised of a number of particles, translational equation of motion of a rigid body is similar to the equation for system of particles, and formulated in global frame as

$$\sum \mathbf{F} = m\, \mathbf{a}_G. \qquad (2.43)$$
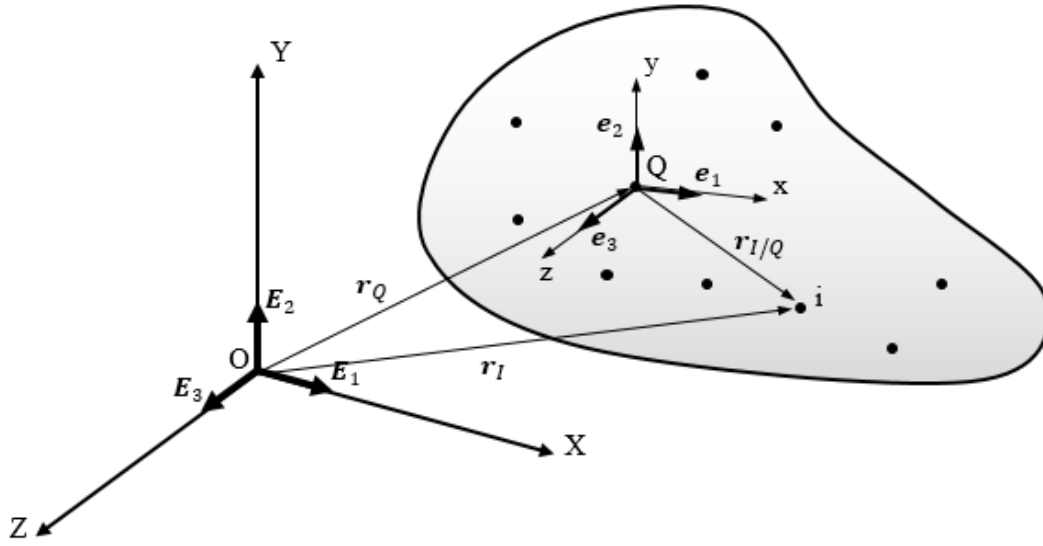
Figure 11. Rigid body in general motion relative to global frame is represented. Local frame is attached to the body at point Q.

Translational equation of motion may be expanded when the body has also a rotational motion. If the body is rotating with the angular velocity $\boldsymbol{\omega}$, and angular acceleration $\dot{\boldsymbol{\omega}}$, translational acceleration in equation (2.43) may be expressed as

$$\boldsymbol{a}_G = \boldsymbol{a}_Q + \dot{\boldsymbol{\omega}} \times \boldsymbol{r}_{Q/G} + \boldsymbol{\omega} \times (\boldsymbol{\omega} \times \boldsymbol{r}_{Q/G}). \tag{2.44}$$

Therefore, translational equation of motion is rewritten as follows

$$\sum \boldsymbol{F}_Q = m\left[\boldsymbol{a}_Q + \dot{\boldsymbol{\omega}} \times \boldsymbol{r}_{Q/G} + \boldsymbol{\omega} \times (\boldsymbol{\omega} \times \boldsymbol{r}_{Q/G})\right], \tag{2.45}$$

where $\boldsymbol{F}_Q = \begin{bmatrix} F_{Qx} & F_{Qy} & F_{Qz} \end{bmatrix}^T$, $\boldsymbol{a}_Q = \begin{bmatrix} a_{Qx} & a_{Qy} & a_{Qz} \end{bmatrix}^T$, $\boldsymbol{\omega} = \begin{bmatrix} \omega_x & \omega_y & \omega_z \end{bmatrix}^T$, $\dot{\boldsymbol{\omega}} = \begin{bmatrix} \dot{\omega}_x & \dot{\omega}_y & \dot{\omega}_z \end{bmatrix}^T$.

That translational equation of motion can also be written by separating into components as

$$\sum F_{Qx} = m\left[a_{Qx} + x(-\omega_y^2 - \omega_z^2) + y(-\dot{\omega}_z + \omega_x\omega_y) + z(\dot{\omega}_y + \omega_x\omega_z)\right],$$

$$\sum F_{Qy} = m\left[a_{Qy} + x(\dot{\omega}_z + \omega_x\omega_y) + y(-\omega_x^2 - \omega_z^2) + z(-\dot{\omega}_x + \omega_y\omega_z)\right], \quad (2.46)$$

$$\sum F_{Qz} = m\left[a_{Qz} + x(-\dot{\omega}_y + \omega_x\omega_z) + y(\dot{\omega}_x + \omega_y\omega_z) + z(-\omega_x^2 - \omega_y^2)\right].$$

20

Similarly, for rotational equation of motion for a system of particles as in Figure 11 may be extended for a rigid body in global frame as

$$\sum M_Q = \dot{H}_Q. \tag{2.47}$$

If the local frame, which is fixed to the body at point Q, has an angular velocity $\boldsymbol{\omega}$, equation (2.47) may be written as follows

$$\sum M_Q = \left(\dot{H}_Q\right)_{xyz} + \boldsymbol{\omega} \times H_Q \tag{2.48}$$

where $\boldsymbol{M}_Q = \begin{bmatrix} M_{Qx} & M_{Qy} & M_{Qz} \end{bmatrix}^T$, $\boldsymbol{\omega} = \begin{bmatrix} \omega_x & \omega_y & \omega_z \end{bmatrix}^T$, $\boldsymbol{H}_Q = \begin{bmatrix} H_{Qx} & H_{Qy} & H_{Qz} \end{bmatrix}^T$, $\dot{\boldsymbol{H}}_Q = \begin{bmatrix} \dot{H}_{Qx} & \dot{H}_{Qy} & \dot{H}_{Qz} \end{bmatrix}^T$.

If equation (2.41) are replaced into equation (2.48) and derivative operations are made, the Cartesian components of the rotational equation of motion is expressed as

$$\sum M_{Qx} = m\left(y\,a_{Qz} - z\,a_{Qy}\right) + I_{xx}\,\dot{\omega}_x - \left(I_{yy} - I_{zz}\right)\omega_y\omega_z$$
$$- I_{xy}\left(\dot{\omega}_y - \omega_x\omega_z\right) - I_{xz}\left(\dot{\omega}_z + \omega_x\omega_y\right) - I_{yz}\left(\omega_y^2 - \omega_z^2\right),$$

$$\sum M_{Qy} = m\left(z\,a_{Qx} - x\,a_{Qz}\right) + I_{yy}\,\dot{\omega}_y - \left(I_{zz} - I_{xx}\right)\omega_x\omega_z \tag{2.49}$$
$$- I_{xy}\left(\dot{\omega}_x + \omega_y\omega_z\right) - I_{xz}\left(\omega_z^2 - \omega_x^2\right) - I_{yz}\left(\dot{\omega}_z - \omega_x\omega_y\right),$$

$$\sum M_{Qz} = m\left(x\,a_{Qy} - y\,a_{Qx}\right) + I_{zz}\,\dot{\omega}_z - \left(I_{xx} - I_{yy}\right)\omega_x\omega_y$$
$$- I_{xy}\left(\omega_x^2 - \omega_y^2\right) - I_{xz}\left(\dot{\omega}_x - \omega_y\omega_z\right) - I_{yz}\left(\dot{\omega}_y + \omega_x\omega_z\right).$$

The equations of motion expressed in equations (2.46) and (2.49) do not include gravitational effects. For more general expressions, gravitational acceleration components in local frame can be added to the translational accelerations in order to include gravitational effects on the body. After this summation is made and $\dot{\omega}$'s are replaced by α's, equations (2.46) and (2.49) may be written in matrix formulation to be shown easily as follows

$$\begin{Bmatrix}\sum F_{Q_x}\\\sum F_{Q_y}\\\sum F_{Q_z}\end{Bmatrix} = m\left(\begin{Bmatrix}a_{Qx}+g_x\\a_{Qy}+g_y\\a_{Qz}+g_z\end{Bmatrix}+\begin{bmatrix}-\omega_y^2-\omega_z^2 & -\alpha_z+\omega_x\omega_y & \alpha_y+\omega_x\omega_z\\\alpha_z+\omega_x\omega_y & -\omega_x^2-\omega_z^2 & -\alpha_x+\omega_y\omega_z\\-\alpha_y+\omega_x\omega_z & \alpha_x+\omega_y\omega_z & -\omega_x^2-\omega_y^2\end{bmatrix}\begin{Bmatrix}x\\y\\z\end{Bmatrix}\right),$$

$$\begin{Bmatrix}\sum M_{Q_x}\\\sum M_{Q_y}\\\sum M_{Q_z}\end{Bmatrix} = m\begin{bmatrix}0 & a_{Qz}+g_z & -a_{Qy}-g_y\\-a_{Qz}-g_z & 0 & a_{Qx}+g_x\\a_{Qy}+g_y & -a_{Qx}-g_x & 0\end{bmatrix}\begin{Bmatrix}x\\y\\z\end{Bmatrix}+\begin{bmatrix}I_{xx} & I_{xy} & I_{xz}\\I_{xy} & I_{yy} & I_{yz}\\I_{xz} & I_{yz} & I_{zz}\end{bmatrix}\begin{Bmatrix}\alpha_x\\\alpha_y\\\alpha_z\end{Bmatrix}$$

$$+\begin{bmatrix}0 & -\omega_z & \omega_y\\\omega_z & 0 & -\omega_x\\-\omega_y & \omega_x & 0\end{bmatrix}\begin{bmatrix}I_{xx} & I_{xy} & I_{xz}\\I_{xy} & I_{yy} & I_{yz}\\I_{xz} & I_{yz} & I_{zz}\end{bmatrix}\begin{Bmatrix}\omega_x\\\omega_y\\\omega_z\end{Bmatrix},$$

(2.50)

where g_x, g_y, g_z are the components of the gravitational acceleration in local frame.

Equations (2.50) are the base equations in order to get mass properties of the body. The bodies whose inertia parameters are to be found throughout the thesis are assumed as a rigid body. Their mass, location of mass center and inertia parameters are going to be calculated using these equations.

m gives the mass of the body. x, y and z give the center of mass location with respect to reference point Q. $I_{xx}, I_{yy}, I_{zz}, I_{xy}, I_{xz}, I_{yz}$ represent the inertia parameters of the body. The inertia parameters are about the reference point Q, since the force, moment, velocity and acceleration vectors are expressed at the point Q.

Generally, it is more convenient to express inertia parameters about the center of mass. Therefore, using parallel axis theorem, obtained inertia parameters can be translated to center of mass location.

2.1.8. Parallel Axis Theorem

Parallel axis theorem states that if inertia parameters about the centroidal axes are known, moment of inertia parameters about any parallel axes can be obtained.
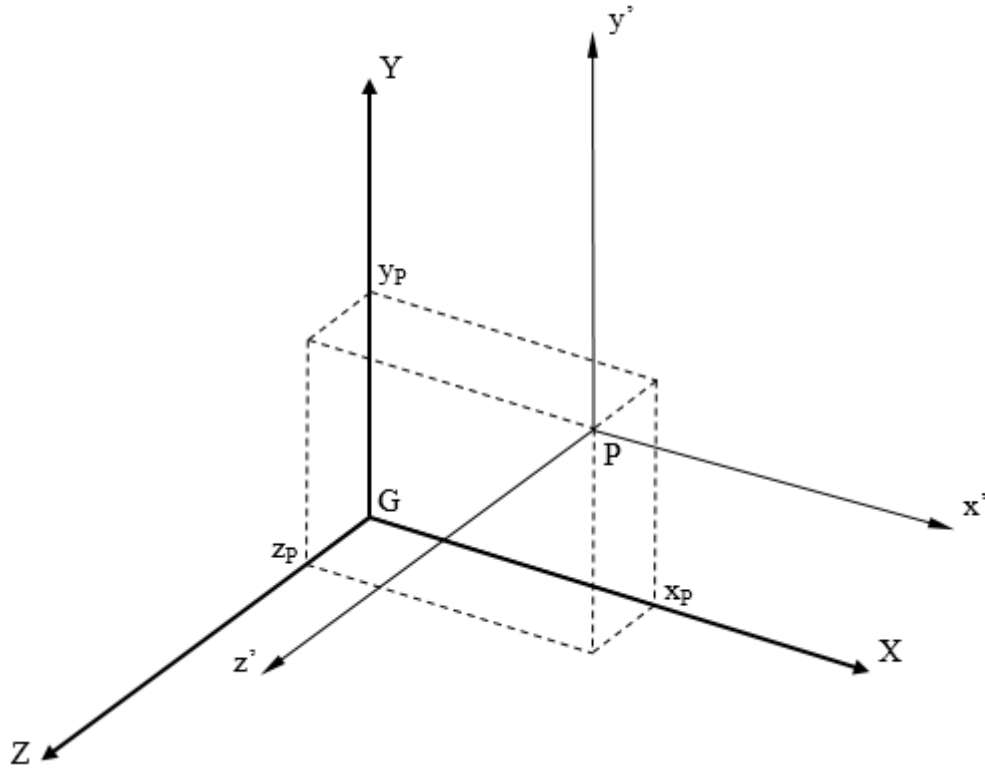
Figure 12. Inertia parameters with respect to center of gravity G and arbitrary point P can be correlated by using parallel distances between their axes.

For the body in Figure 12, the relation between inertia parameters about local axes located at center of mass, G, and another parallel axes located at point P can be expressed using parallel axis theorem as follows

$$[I_P] = [I_G] + m \begin{bmatrix} y_p^2 + z_p^2 & -x_p y_p & -x_p z_p \\ -x_p y_p & x_p^2 + z_p^2 & -y_p z_p \\ -x_p z_p & -y_p z_p & x_p^2 + y_p^2 \end{bmatrix}. \tag{2.51}$$

where $[I_G]$ is inertia tensor about centroidal axes and $[I_P]$ is inertia tensor about parallel axes located at point P.

2.1.9. Moment of Inertia About an Arbitrary Axis

If the inertia parameters about the reference frame of the body shown in Figure 13 is known, inertia parameters about an arbitrary axis, a, passing through point O can be derived.
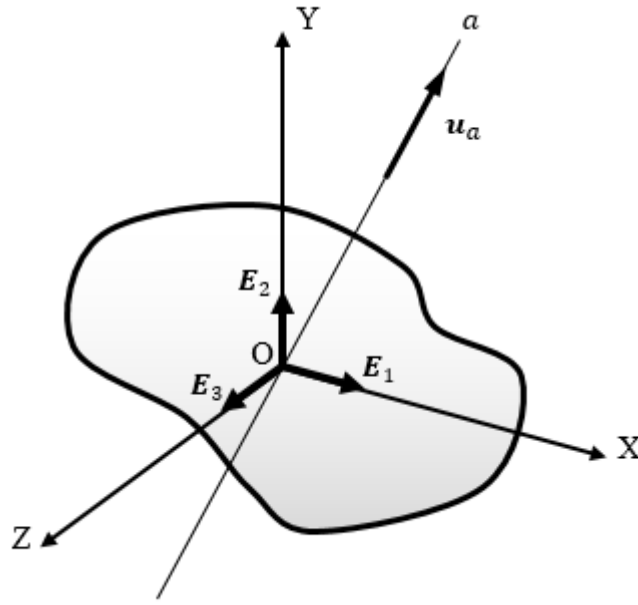
Figure 13. Representation of an arbitrary axis passing through origin of the reference frame.

The direction of the arbitrary axis, a, is defined by the unit vector $\boldsymbol{u}_a$ as in 2.48

$$\boldsymbol{u}_a = \cos\alpha\ \boldsymbol{E}_1 + \cos\beta\ \boldsymbol{E}_2 + \cos\gamma\ \boldsymbol{E}_3. \tag{2.52}$$

where $\cos\alpha$, $\cos\beta$ and $\cos\gamma$ are the direction cosines. The moment of inertia about the arbitrary axis, a, can be obtained in terms of inertia parameters about reference frame as

$$\begin{aligned} I_a = {} & I_{xx}\cos^2\alpha + I_{yy}\cos^2\beta + I_{zz}\cos^2\gamma \\ & - 2\,I_{xy}\cos\alpha\cos\beta - 2\,I_{yz}\cos\beta\cos\gamma \\ & - 2\,I_{xz}\cos\alpha\cos\gamma. \end{aligned} \tag{2.53}$$

2.1.10. Principal Moments of Inertia [3], [4]

Inertia tensor given in equation (2.41) is in the following form

$$I = \begin{bmatrix} I_{xx} & -I_{xy} & -I_{xz} \\ -I_{xy} & I_{yy} & -I_{yz} \\ -I_{xz} & -I_{yz} & I_{zz} \end{bmatrix}. \tag{2.54}$$

The inertia tensor depends on the location and orientation of the reference coordinate system. Therefore, there is a reference coordinate system which is located at center of gravity of the body and makes the inertia tensor diagonal as follows

$$I^* = \begin{bmatrix} I_x^* & 0 & 0 \\ 0 & I_y^* & 0 \\ 0 & 0 & I_z^* \end{bmatrix}. \tag{2.55}$$

where I_x^*, I_y^*, I_z^* are the principal moments of inertia of the body for the principal axes of inertia $(x^* y^* z^*)$. Using the principal moments of inertia simplifies the rotational equations of motion in (2.49) and regarding calculations.

The principal axes and the corresponding moments of inertia can be calculated by solving the following eigenvalue problem

$$([I] - \lambda[I_0])[u^*] = 0. \tag{2.56}$$

where $[I_0]$ is an identity matrix, λ is the eigenvalues of the inertia matrix $[I]$, and $[u^*] = [\{u_1^*\} \quad \{u_2^*\} \quad \{u_3^*\}]$ is the eigenvectors of the inertia matrix $[I]$.

In order to find the principal moments of inertia, the following equation should be solved

$$det([I] - \lambda[I_0]) = 0. \tag{2.57}$$

Solution of equation (2.57) gives the principal moments of inertia, $\lambda = I_x^*, I_y^*, I_z^*$ and the solution of equation (2.56) gives the unit direction vectors $(\{u_1^*\}, \{u_2^*\}, \{u_3^*\})$ for each principal axes. However, one of the three equations in equation (2.56) is linearly dependent to others. Thus, one component of a direction vector should be chosen

arbitrarily and the other components are found in terms of it. If it is considered that the direction vector is a unit vector, the following additional equation can be written

$$\{u_i^*\}^T * \{u_i^*\} = 1. \tag{2.58}$$

Using that additional equation leads to find eigenvectors (direction vectors) uniquely. the obtained eigenvectors form an orthogonal set. Proof of this property can be examined in [4].

2.2. LITERATURE OVERVIEW

In the literature, there are numerous resources investigating the measurement of mass properties. The methods in the literature can be mainly divided into two categories: static methods and dynamic methods. In static methods, the specimen whose mass parameters are to be measured is in a stationary position while the measurements are being done. These static methods cannot provide all the mass parameters, they can only measure the mass and center of gravity locations. In dynamic methods, the test specimen has a motion in space. Besides the mass and center of gravity locations, inertia parameters are also measured in dynamic methods using equations of motion.

Measuring the mass is an ordinary procedure by using a weighing machine or a load sensor. The main task is to obtain center of gravity locations and inertia parameters. The most basic way to get center of gravity locations is hanging method in which the test specimen is hanged with a wire [5]–[8]. When the specimen comes into stationary position, the axis of the wire crosses through center of gravity. Repeating the same procedure at least one more time enables to get center of gravity locations geometrically.

Balancing method is also used to get center of gravity positions [6], [9], [10]. The test specimen is placed on a lever and the lever is balanced with a known force acting on the specified location. Since the position of rotation center and the position at where the force acts is known, the location where the specimen's gravitational force acts can

be calculated using moment balance equations. Replacing the specimen on the lever with at least three different orientations gives center of gravity locations geometrically.

Another static method to obtain center of gravity locations is the force measurement method. In this method, the test specimen is placed on at least three force sensors [11], [12]. The summation of the readings from the force sensors gives the mass of the specimen. Center of gravity can be calculated by taking the moment of the forces on the sensors and the gravitational force of the specimen about any point. This gives two center of gravity positions. Changing the orientation of the specimen and writing moment equations about any point again are required to obtain the remaining center of gravity location.

In dynamic methods, rotational equations of motion are used. Generally, these equations are simplified to one dimensional case to ease the measurement procedure. However, this simplification results in the need for more than one test configuration. In the cases where no simplification is done and three dimensional general motion is applied, one test configuration is enough to obtain all mass parameters.

The simplest dynamic method is the pendulum method. The mass and the center of gravity locations should be known in advance in this method. There should be an oscillatory rotational motion about one axis and a restoring force. Equations of oscillatory rotational motion about one axis is used to calculate moment of inertia about the rotation axis. Pendulum method can be separated into groups with the type of the restoring force. The restoring force may be gravitational force or a spring force. In gravitational pendulum methods [5], [8], [13]–[15], gravitational force is used as a restoring force. The test specimen is hanged to create a swinging motion, and the period of the oscillations are measured. Then, the geometric dimensions and the measured period of oscillations are related to natural frequency appearing in the equation of motion. Then, the moment of inertia value is calculated. Parallel multifilar pendulum method is another method that uses gravitational force as a restoring force [8], [16]–[24]. In this method, the test specimen is placed on a plate which is hanged with two or more cables. Center of gravity location should be located in the vertical

axis of the geometric center of the cables. Small angular displacement about that axis is supplied and the specimen makes an oscillatory motion. Again, by measuring the period of oscillations, moment of inertia about rotation axis is reached. Spring force is another option for the restoring force of the pendulum method. The spring can be a linear spring [10], [25]–[29], or a torsional spring [30], [31]. The specimen is attached in a configuration such that when an initial displacement is given, it makes a rotational oscillatory motion. Similar to the gravitational pendulum method, equations of oscillatory motion are composed and period of oscillations are measured. Then by relating the natural frequency of the system with the spring constant, moment of inertia about rotation axis can be calculated. In all the alternatives of the pendulum method, only one moment of inertia parameter can be calculated for a single measurement. Therefore, at least six different configurations and measurements are required to obtain all inertia parameters.

Run-down method directly uses the rotational equations of motion in one axis to obtain moment of inertia value about that axis [5]. The test specimen is forced to rotate about one axis with a variable rotational velocity. Acceleration and moment about the rotation axis is measured and replaced into rotational equations of motion. By doing this, moment of inertia about rotation axis can be calculated. In order to obtain the rest of the inertia parameters, the test should be repeated with five more orientation of the specimen.

In the literature, there exists some methods to eliminate the need of the changing the configuration of the test setup. Main idea in these multifaceted methods is to provide three dimensional rotational motion to the test specimen in a single configuration. Non-parallel multifilar pendulum may be used to create three dimensional rotational motion [32], [33]. The test specimen is connected to a frame which is hanged with three or four non-parallel cables. By means of that configuration, three dimensional swinging motion occurs inherently if an initial displacement is given to the specimen. Measuring the motion and the forces acting on the specimen and replacing them into the rotational equations of motion give a chance to derive all the mass properties of the specimen in a single configuration.

Three dimensional rotational motion can also be generated with the help of actuators. In the methods that uses dynamic actuators, forces acting on the specimen and the motion of the specimen are recorded [34]–[40]. These recordings are replaced into rotational equations of motion, and complex mathematical procedure is applied in order to obtain all ten inertia parameters simultaneously similar to the non-parallel multifilar pendulum method.

The methods described thus far uses all the measurements in the time domain. Mass properties can also be measured by using the kinematic and kinetic values in frequency domain. The modal methods mentioned in [41], [42], [51]–[60], [43], [61]–[63], [44]–[50] are the most popular method to obtain mass properties in the frequency domain. In these methods, the specimen is placed on a softly supported fixture as it can move in quasifree-free condition. The force is applied to the specimen and accelerations of different points on the specimen are measured. Using these acceleration measurements, mode shapes of the body is estimated. Then, orthogonality relation between mass matrix and the mode shapes are used to derive all the mass parameters simultaneously.

Another method to obtain mass properties in frequency domain is the inertia restrained method [41], [42], [46], [50], [52], [57], [61], [64], [65]. As in the modal method, the specimen is placed on a softly supported fixture. The specimen is excited at different locations with different frequencies by known forces and accelerations at different locations on the specimen are measured. The measurement of the mass properties is accomplished in two steps. In the first step, mass and the center of gravity locations are measured. In the second step, inertia parameters are calculated.

The methods requiring at least one configuration change to obtain mass parameters are explained in Simple Methods section (2.2.1). The methods that can measure all the mass parameters in a single configurations are expressed in details in Multifaceted Methods section (2.2.2).

2.2.1. Simple Methods

2.2.1.1. *Static Methods*

In static methods, the specimen whose mass parameters are to be measured is in a stationary position. Therefore, velocity and acceleration terms disappear from the equations (2.50), and they get into the following form

$$
\begin{Bmatrix} \Sigma F_x \\ \Sigma F_y \\ \Sigma F_z \end{Bmatrix} = m \begin{Bmatrix} g_x \\ g_y \\ g_z \end{Bmatrix},
$$

$$
\begin{Bmatrix} \Sigma M_x \\ \Sigma M_y \\ \Sigma M_z \end{Bmatrix} = m \begin{bmatrix} 0 & g_z & -g_y \\ -g_z & 0 & +g_x \\ g_y & -g_x & 0 \end{bmatrix} \begin{Bmatrix} x \\ y \\ z \end{Bmatrix}.
$$

(2.59)

As seen in equation (2.59)$_b$, inertia parameters also disappear. That is why static methods are only able to measure mass and center of mass locations. They cannot measure inertia parameters of the test specimen.

2.2.1.1.1. Hanging Method [5]–[8]

In the suspension method, mass and the center of gravity positions of the test specimen can be determined. The test specimen is hung with a wire from the ceiling or the test frame, etc. and then it comes into equilibrium as seen in the Figure 14.
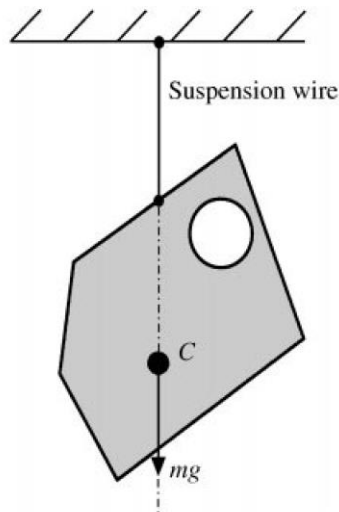
Figure 14. Configuration for hanging method. Wire direction points out the center of gravity location. [66]

30

Mass of the specimen may be found by the use of a force sensor at the wire or by a simple weighing machine. When the specimen is hung and come into the equilibrium position, the wire direction crosses through the center of gravity location of the specimen. In order to get all the center of gravity positions, the hanging process must be repeated at least two times. In the first measurement, center of gravity positions in one plane, which is the parallel to the ground, can be determined. To get the third center of gravity position, i.e. the center of gravity height, the test specimen should be hung one more time by changing the connection point of the wire. Then, the intersection of these two wire directions indicates the center of gravity position.

Despite the hanging method is a very simple method, it does not point out the center of gravity locations numerically. It only provides geometric information. Therefore, it can be said that the accuracy of this method is low. Requirement for replacement of the specimen is another unfavorable side of this method.

2.2.1.1.2. Balancing Method [6], [9], [10]

Balancing method determines the center of gravity locations. The mass of the test specimen should be found in advance. In this method, test specimen is located on an edge pretending as a revolute joint. The specimen is held at another position as in Figure 15. Then using moment balance equations about the edge, center of gravity position along horizontal axis may easily be calculated.
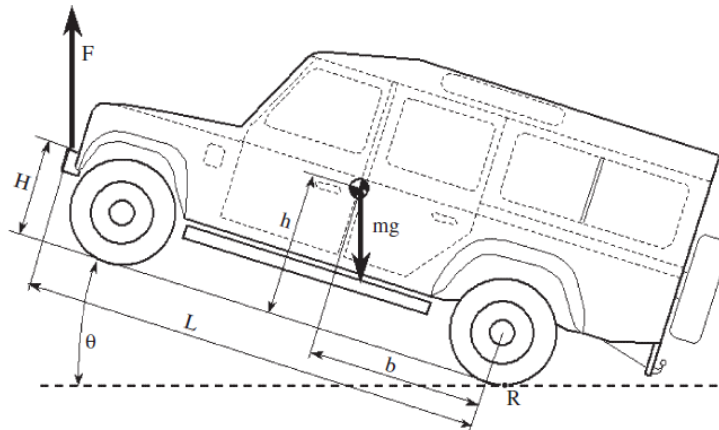
Figure 15. The specimen can rotate about point R. The distance, b, is calculated using moment balance about point R. [10]

A lever may also be used for balancing method. For this case, the specimen is placed at the one side of the lever, and a counterweight with a known mass is used to balance the lever as in the Figure 16. Similarly, location of the center of gravity position along vertical axis may be calculated with moment balance equations.
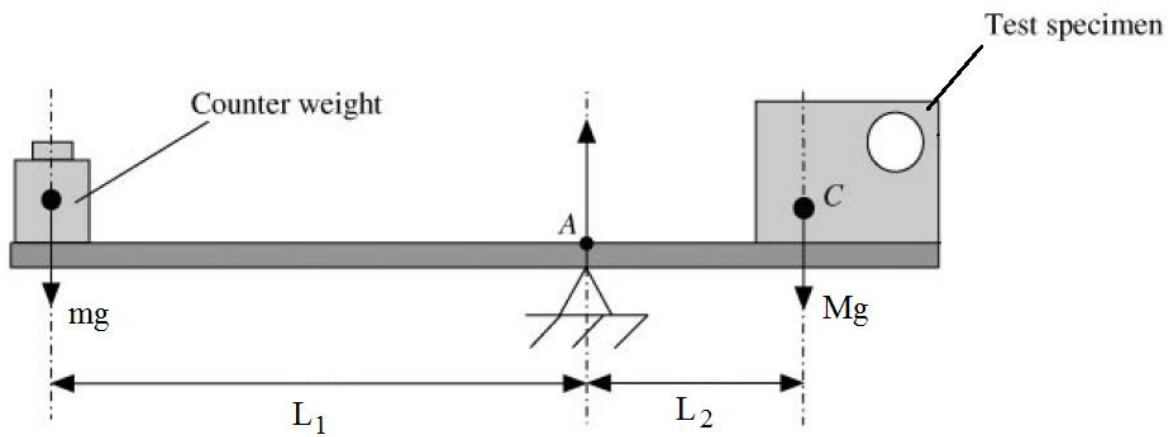
Figure 16. Moment balance about point A is used to find the distance between center of gravity position along vertical axis and point A, L_2. [66]

Calculation of the center of gravity positions along the other axes requires two more measurements. The test specimen should be rotated and the same procedures should be performed to describe all the center of gravity positions.

Balancing method is a simple and successful method with better accuracy for center of gravity locations relative to hanging method. However, necessity of three setup process is the inappropriate site of this method.

2.2.1.1.3. Force Measurement Method [11], [12]

In this method, the distribution of forces arise from gravity of the body are utilized. First, the body should be placed on a plate which is supported at least three different points as in the Figure 17. The forces in vertical direction at these support points are measured. The mass of the body is found from the summation of the readings. For the gravity locations, moment equilibrium equations are used. The gravity locations on the plane parallel to the ground is calculated firstly. Then the orientation of the body is changed, and the new moment equations are constituted and solved. By this way, the remaining gravity position may be obtained.

The third gravity locations may be found with a different method. If the plate is tilted with a known angle while the body is still attached to it, the moment equations may be rewritten using geometrical relations. Since the first two gravity locations are fixed by the previous moment equilibrium, the last gravity location is obtained.
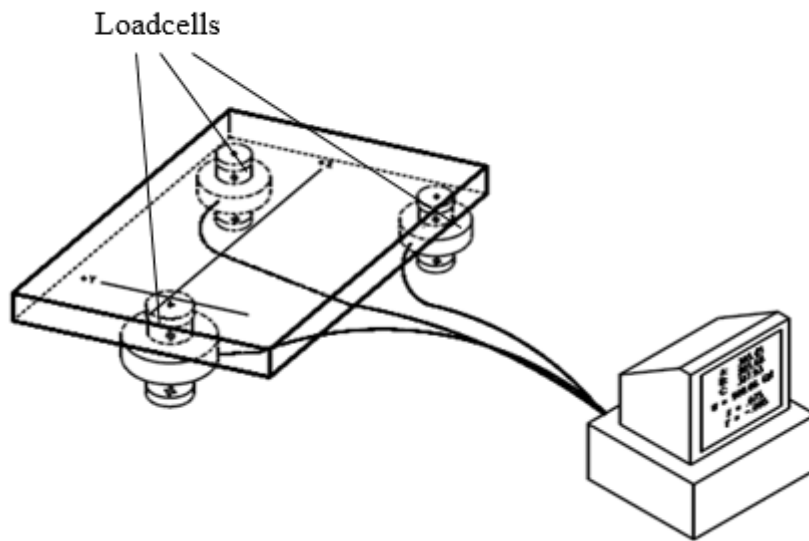
Figure 17. Test specimen is placed on the plate shown and arising forces are measured. [12]

Force measurement method is also a simple and accurate method; however, at least two configuration necessity is handicap for this method.

2.2.1.2. *Dynamic Methods*

In dynamic methods, the test specimen has a motion in space. Besides the mass and center of mass locations, inertia parameters are also measured in dynamic methods using equations (2.50).

2.2.1.2.1. **Pendulum Method** [5], [8], [20]–[29], [10], [30], [31], [13]–[19]

In the pendulum method, there is an oscillatory motion created by an initial displacement and a restoring force. Restoring force may be gravitational force or a spring force.

One alternative of a pendulum method is a gravitational pendulum. The body whose mass properties are to be measured is hanged with a revolute joint as shown in Figure 18. As in the hanging method, mass and center of mass locations are found. To find inertia parameters, a small angular displacement, θ, is given to the body. Then, the body makes a swinging motion while the gravity acts as a restoring force.
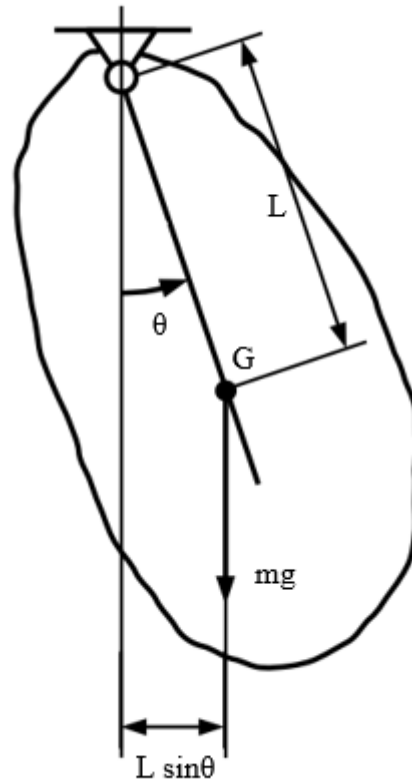
Figure 18. Initial displacement, $\boldsymbol{\theta}$, is given to the specimen and gravitational force tries to bring the specimen to the equilibrium.

For the system in the figure, equation (2.50)_b simplifies to equation (2.59)_b if it is written about rotation center, and no rotational motion exists about y and z axes

$$\Sigma M_x = I_{xx}\,\dot{\omega}_x. \tag{2.60}$$

The total moment expression in equation (2.59)_b is due to the gravity only, and may be formulated as $M = -mg\,L\sin\theta$. Since small angular displacement is assumed, the simplification, $\sin\theta \cong \theta$, can be made in the moment equation. Then, ignoring the subscripts, the equation is rewritten as follows

$$I\ddot{\theta} + mgL\,\theta = 0. \tag{2.61}$$

Equation (2.61) may be written in the form of $\ddot{\theta} + \dfrac{mgL}{I}\theta = 0$, which is the general form of equation of an oscillatory motion. The term $\dfrac{mgL}{I}$ is equal to the square of

natural frequency of the system, ω_n^2, and it can also be expressed as $\omega_n = 2\pi f = \frac{2\pi}{T}$ where f is the oscillation frequency and T is the oscillation period. If the oscillation period of the body is measured after the given initial angular displacement, inertia about the rotation axis may be found as follows

$$I = \frac{mgLT^2}{(2\pi)^2}.$$ (2.62)

An alternative way of pendulum method is a parallel multifilar pendulum. In this method, the body is suspended by two or more cables which are parallel to each other. Three cables configuration is shown in the Figure 19.
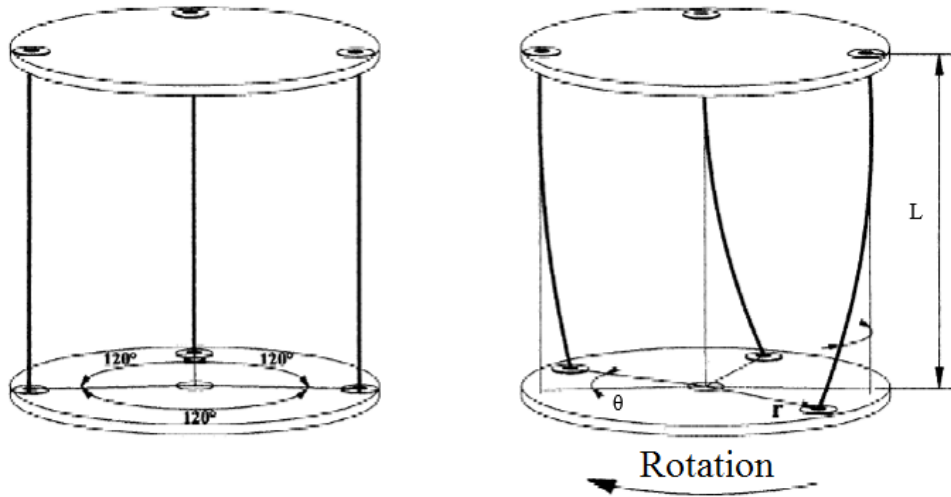
Figure 19. Test specimen is placed on the plate shown and initial angular displacement is given. [31]

When small initial angular displacement is also given to this system and the body starts to oscillate about the vertical axis. Here, the gravity has the restoring effect. If the small angular displacements are assumed, the moment about the rotation axis is obtained as $M = -\frac{mgr^2}{L}\theta$. Then, the equation of motion may be written as follows

$$I\ddot{\theta} + \frac{mgr^2}{L}\theta = 0.$$ (2.63)

where r is the distance between center of plate and connection point of the cable to the plate, L is the length of cables. Again, equation (2.63) is in the form of equation of motion of an oscillator. Approving that $\omega_n^2 = \frac{mgr^2}{IL}$, and measuring the period of oscillations, inertia about the rotation axis is obtained as follows.

$$I = \frac{mgr^2 T}{(2\pi)^2 L}.$$
(2.64)

In the multifilar pendulum method, mass center of the body should be placed on the rotation axis which is the center of the cables. Therefore, as in the torsional pendulum method, mass center position should be known previously.

Another alternative of the pendulum method is linear spring pendulum method. In this method, the specimen is placed on a knife edge and a linear spring is attached to it as shown in Figure 20. When an initial displacement is given to the specimen, rotational oscillatory motion about knife edge is obtained.
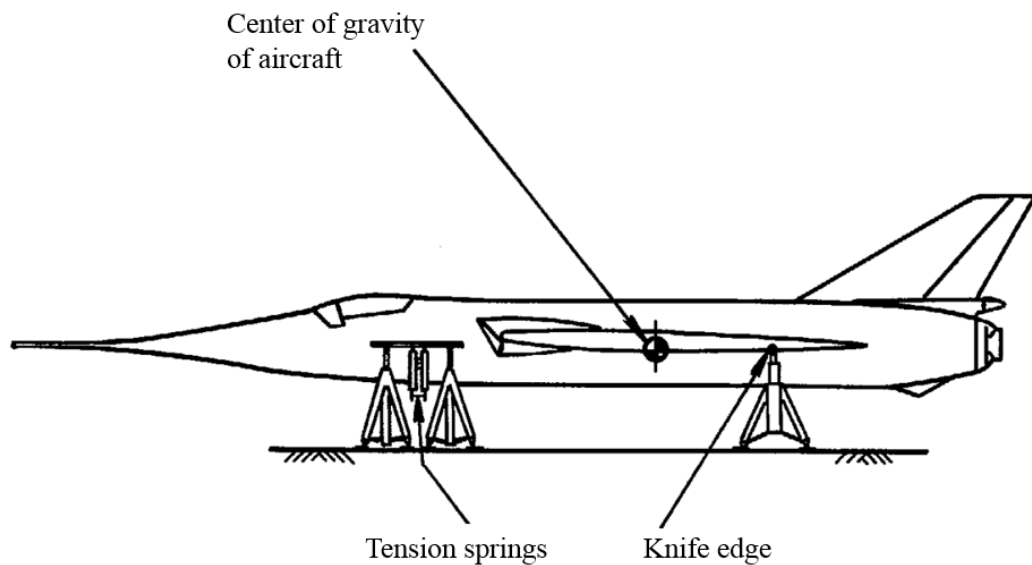
Figure 20. Tension springs acts as a restoring force and creates an oscillatory rotational motion about knife edge. [26]

Instead of linear spring, a rod with low torsional stiffness or a torsional spring can also be used. Therefore, torsional stiffness of a rod or a spring is used as a restoring force.

In this method, the body is attached to the rod and it can only rotate about the vertical axis as shown in Figure 21.
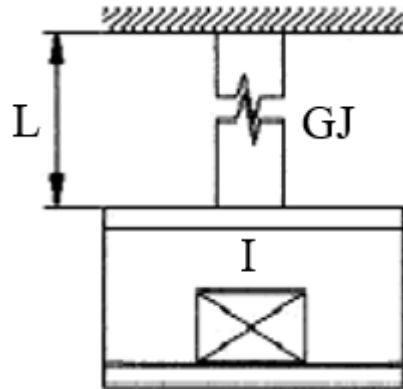
Figure 21. The test specimen is attached to the ceiling with a rod. Torsional stiffness of the rod is found by the formula $k = GJ/L$. [31]

For both case where linear or torsional spring is used, when an initial angular displacement is given to the body, it makes an oscillatory rotational motion. Similar to the equation (2.61), equation of motion for this system is written as

$$I\ddot{\theta} + k\theta = 0. \qquad (2.65)$$

where, k is the spring constant. Equation (2.65) is also in the form of an equation of motion of oscillator. This time, natural frequency of the oscillator is written as $\omega_n^2 = k/l$. Again, if the period of oscillations is measured, the inertia about the rotation axis may be found by the following equation

$$I = \frac{k\,T^2}{(2\pi)^2}. \qquad (2.66)$$

Using linear spring or torsional spring pendulum method, mass and the center of mass locations cannot be obtained. Therefore, these parameters should be known beforehand. Then, inertia about center of gravity can be found by using parallel axis theorem.

In all alternatives of the pendulum method, inertia parameters are calculated about the rotation axis. Inertia parameters about center of gravity may be derived using parallel axis theorem as in equation (2.51).

In pendulum methods, only one inertia parameter can be found in a single configuration. In order to get the other inertia parameters, orientation of the body should be changed and the same process should be repeated five more times. By doing this, six moment of inertia parameters about six different axes is obtained. Then, using equation (2.52), all inertia parameters of the body can be calculated by constructing six different equations.

Using small angular displacements increases the accuracy of pendulum method. In addition to that, accuracy of this method depends on the measuring the period of oscillations correctly.

2.2.1.2.2. Run-Down Method [5]

In the run-down method, the body, whose inertia parameters are to be measured, is forced to rotate about one axis with a non-zero angular acceleration.

The moment occurred between the body and actuator is measured during the rotational motion. Since there is a rotational motion about only one axis, equation of motion in equation (2.50)$_b$ again simplifies to the following form

$$\Sigma M_x = I_{xx}\, \dot{\omega}_x. \qquad (2.67)$$

Ignoring the subscripts, inertia about the rotation axis can be calculated as the ratio of the torque to the rotational acceleration as follows

$$I = M / \dot{\omega}. \qquad (2.68)$$

The rotational axis does not have to cross the mass center. If the inertia about axis passing through mass center is desired, parallel axis theorem should be applied. Also in run-down method, mass and mass center should be known previously. In this method, inertia about only one axis is found. Therefore, orientation of the body should

be changed and same procedure should be applied six times. The accuracy of this method depends on the correct measurement of the torque and a proper acceleration input. If the losses at the actuator and connections are kept low, run-down method gives satisfactory results.

2.2.2. Multifaceted Methods

2.2.2.1. *Time Domain Methods*

2.2.2.1.1. Non-Parallel Multifilar Pendulum Method [32], [33]

In non-parallel multifilar pendulum method, the body is placed on a fixture which is hanged by at least three non-parallel cables as shown in Figure 22.
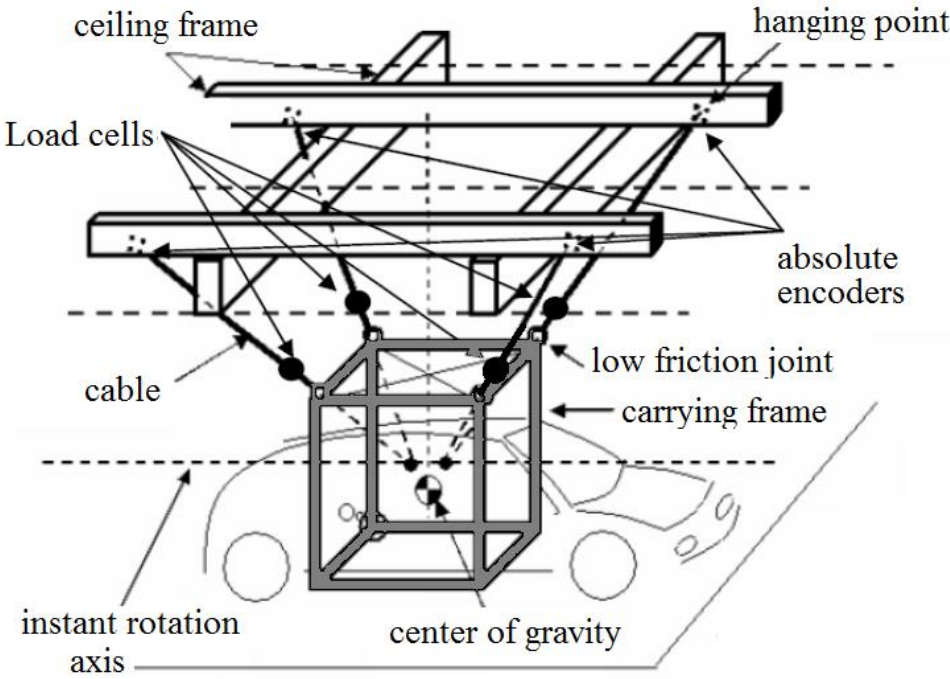
Figure 22. The test specimen is hanged with four non-parallel cables. [33]

Since the cables are not parallel, the body is able to make general three-dimensional motion. If an initial displacement or initial velocity is given to the body, it starts to make a general motion freely. Translational and rotational velocities and accelerations of the body are measured by accelerometers or encoders. Also, the forces occurring on the cables are measured by using load cells. These measurement results are obtained

continuously during the motion, therefore there are values for velocities, accelerations, forces and moments about the measurement point at every time instant.

If these measurements are used in equation (2.50)$_a$, the mass and center of mass locations can be obtained. If they are replaced into equation (2.50)$_b$, all mass parameters, including mass, center of mass locations and inertias, can be found instantaneously.

This method is a simple method to measure mass parameters, because it does not need actuators. Therefore, this method may be easily used for large bodies without increasing the cost too much. Moreover, this method is able to measure all mass parameters in a single configuration with a high accuracy.

2.2.2.1.2. Dynamic Actuator Method [34]–[40]

In the dynamic actuator method, the body is fixed to the test frame. This frame is placed on a mechanism, which can rotate the frame about three orthogonal axes, as shown in Figure 23. By this way, the body is able to rotate an arbitrary axis whose rotation center is known.

Figure 23. The actuator configuration rotates the specimen about point P, and forces and accelerations are measured. [35]

41

The forces and moments acting on the frame are measured. Therefore, moments about any point can be calculated. Angular velocities and accelerations can be measured from the motion of the frame by using accelerometers. Similar to the non-parallel multifilar pendulum method, these kinematic measurement results and moment values can be replaced into the equation (2.50)$_b$. Then, all the mass parameters can be obtained simultaneously.

In this method, static measurements may be applied to get mass and center of mass locations without changing the test configuration. In order to do this, the forces on the actuators are measured at two different orientations of the test frame. Since the measurements are made statically, angular velocities and accelerations vanish from the rotational equations of motion. Therefore, using the load measurements, mass and center of mass locations can be obtained as in the force measurement method.

Although the logic behind this method is similar to the non-parallel multifilar pendulum method, it is more complicated and costly system due to the need of actuator mechanism. However, since the rotation point is known, solution procedure of the rotational equations of motion is easier. This method can provide all mass parameters in a single configuration. The accuracy of this method is strongly affected by the losses occurring on the actuator mechanism. Therefore, if the losses on the actuators are kept minimum, this method gives accurate results.

2.2.2.2. *Frequency Domain Methods*

In time domain methods, kinetic and kinematic values are measured with respect to time. In frequency domain methods, these kinetic and kinematic values are used with respect to frequency. The transformation between time domain and frequency domain can be applied using Fourier Transform as follows [67]

$$F(\omega) = \int_{-\infty}^{+\infty} f(t)\, e^{-i\omega t}\, dt\,,$$

$$f(t) = \frac{1}{2\pi} \int_{-\infty}^{+\infty} F(\omega)\, e^{i\omega t}\, d\omega. \tag{2.69}$$

2.2.2.2.1. Modal Method [41], [42], [51]–[60], [43], [61]–[63], [44]–[50]

In modal method, the body is placed on a softly supported fixture so that it can vibrate spatially, when a force is applied to the body as in Figure 24.
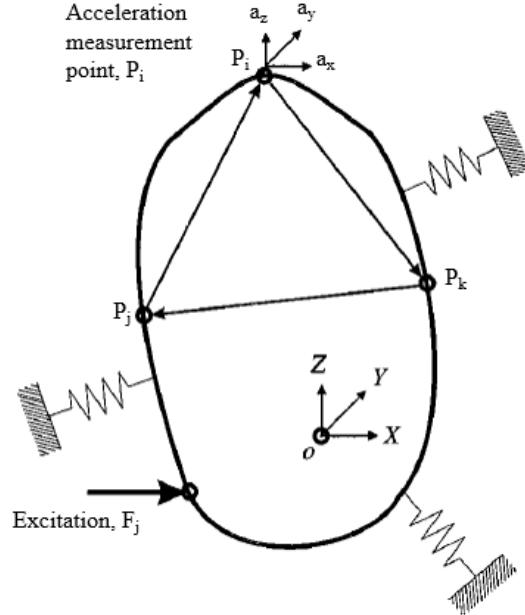
Figure 24. The specimen is placed on springs and makes a general motion with the excited force. [52]

There are some measurement points, whose accelerations are to be measured, on the body. These translational acceleration measurements at different points allows to observe the motion of the body. Natural frequencies, damping ratios and mode shapes of the system are estimated. The estimated mode shape matrix is converted to the mass-normalized mode shape matrix. Then, orthogonality relation between the mass matrix and mode shapes enables to get mass parameters of the body

$$
[\Phi]^T [M] [\Phi] = [I],
$$
$$
[M] = [\Phi]^{-T} [\Phi]^{-1}.
$$

(2.70)

where $[\Phi]$ is the mass-normalized mode shape matrix, $[M]$ is the rigid body mass matrix and $[I]$ is the identity matrix. Mass matrix $[M]$ contains all mass parameters and can be expanded as follows

$$M = \begin{bmatrix} m & 0 & 0 & 0 & mz & my \\ 0 & m & 0 & -mz & 0 & mx \\ 0 & 0 & m & -my & -mx & 0 \\ 0 & mz & my & I_{xx} & -I_{xy} & -I_{xz} \\ -mz & 0 & mx & -I_{xy} & I_{yy} & -I_{yz} \\ -my & -mx & 0 & -I_{xz} & -I_{yz} & I_{zz} \end{bmatrix}. \tag{2.71}$$

where x, y, z are the locations of the center of mass in x, y, z axes. Therefore, solution of equation (2.70) gives mass properties of the body.

In this method, mass parameters are obtained by a single test setup. The body should be excited at different locations and different directions to excite all six rigid body. However, this may be difficult in practice.

2.2.2.2.2. Inertia Restrained Method [41], [42], [46], [50], [52], [57], [61], [64], [65]

In the inertia restrained method, the body is suspended with springs or soft cords in order to simulate free-free boundary condition. Equations of motion for that system is constructed with respect to a given reference point. The body is excited at different locations with different frequencies and its dynamic response is analyzed in a low frequency region by a constant term called as inertia restraint. That method is suitable for the cases in which the rigid body modes and flexible modes are well separated.

Measuring the complete mass parameters is overcome in two steps. In the first step, mass and center of mass locations are calculated using translation equation of motion equation (2.50)ₐ with zero velocities as follows

$$\Sigma \boldsymbol{F} = m \left[\boldsymbol{a}_Q + \dot{\boldsymbol{\omega}} \times \boldsymbol{r}_{Q/G} \right]. \tag{2.72}$$

Center of gravity locations are the unknowns to be solved. Once these unknowns are solved, the second step starts to find inertia parameters. Since the mass and center of mass locations are known from first step and velocities are zero, rotational equations of motion about the mass center get into a simple form as

$$\Sigma M_x = I_{xx}\,\dot{\omega}_x - I_{xy}\,\dot{\omega}_y - I_{xz}\,\dot{\omega}_z,$$

$$\Sigma M_y = I_{yy}\,\dot{\omega}_y - I_{xy}\,\dot{\omega}_x - I_{yz}\,\dot{\omega}_z, \qquad (2.73)$$

$$\Sigma M_z = I_{zz}\,\dot{\omega}_z - I_{xz}\dot{\omega}_x - I_{yz}\,\dot{\omega}_y.$$

Using these equations, inertia parameters about the mass center are calculated. The solution of this method is easy because it gives mass properties with solving linear equations. The inertia restrained method gives the complete mass properties with a single test setup in two steps. The selection of excitation points and acceleration measurement points strongly affect the accuracy of the results. In [67], there is a statistical analysis to minimize the error of inertia restrained method by changing the selection of acceleration measurement points and excitation points/directions.

CHAPTER 3

METHODOLOGY

3.1. DESIGN

3.1.1. Design Selection

The purpose of the design is the measurement of complete mass parameters in a single test. In order to achieve this, a design is selected by utilizing the concepts in the literature given in Chapter 2. Main concepts are based on the use of equations of motion. The equations of motion contain kinematic quantities (positions, velocities, accelerations) and kinetic quantities (forces, moments). Therefore, these quantities should be different from zero to use in equations of motion and in all the concepts, these quantities are desired to be measured.

The selected design is shown in Figure 25 and Figure 26. In that design, the test model is able to make an oscillatory rotational motion about point O. This rotational motion creates translational and rotational velocities and accelerations on the center of gravity of the specimen. Velocities and accelerations are measured from the rotational motion about coordinate axes. In addition, forces and torques created due to the oscillatory motion are measured at point Q.

Simplicity of that design is the main advantage of the test device. It does not require complicated actuators to move the system. An initial displacement is enough to create a rotational motion. Also, since the forces and torques are measured at point Q, these measurements do not include the effects of the parts above the load cell, which are the nested frames, extension link, torsional spring, encoders and cables. Also, the frictional losses in these parts are eliminated. Furthermore, that design can be used for heavy masses by only changing the dimensions and the capacity of the load cell.
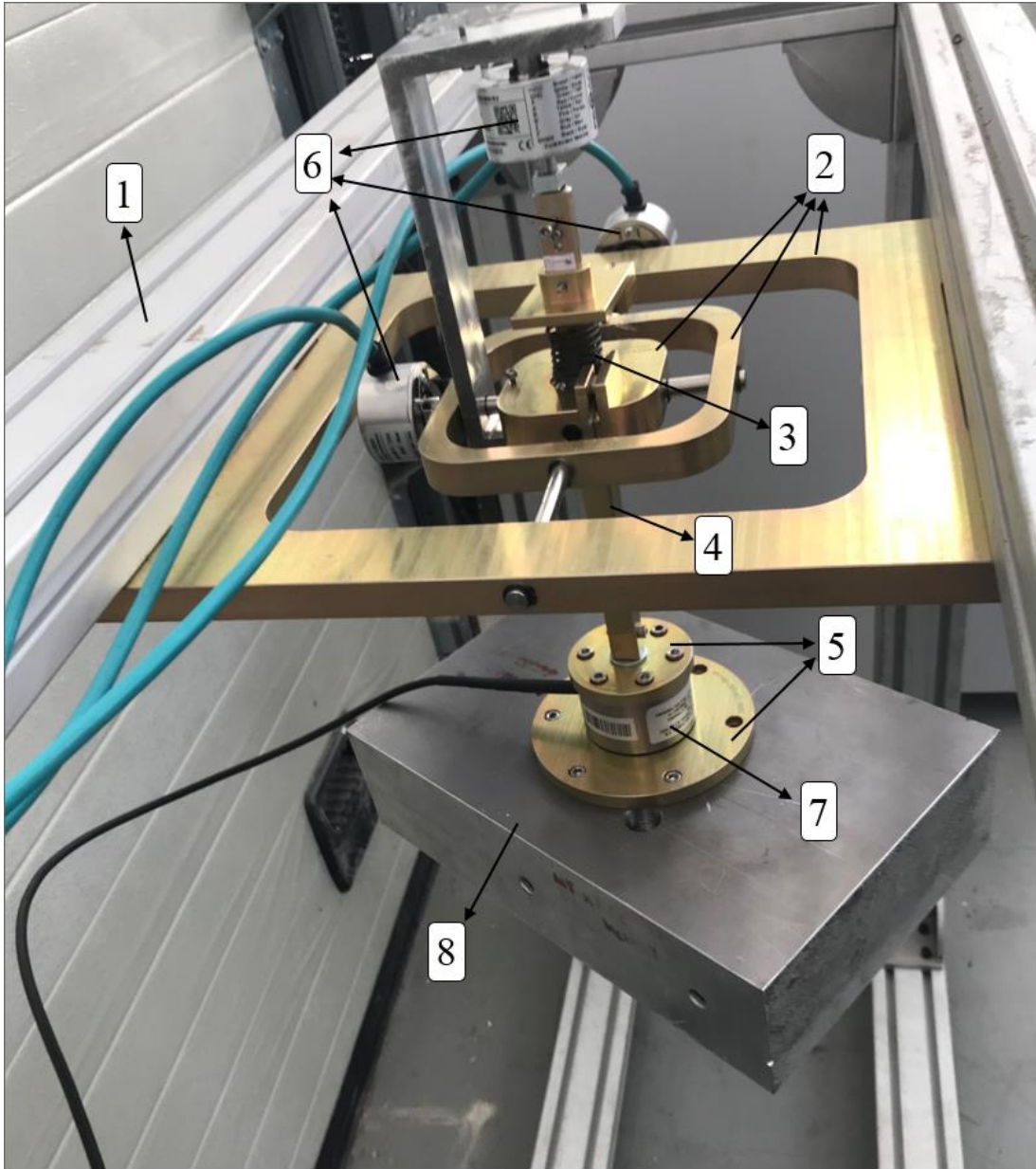
Figure 25. The configuration of test device is given. Main parts of the system are numbered.
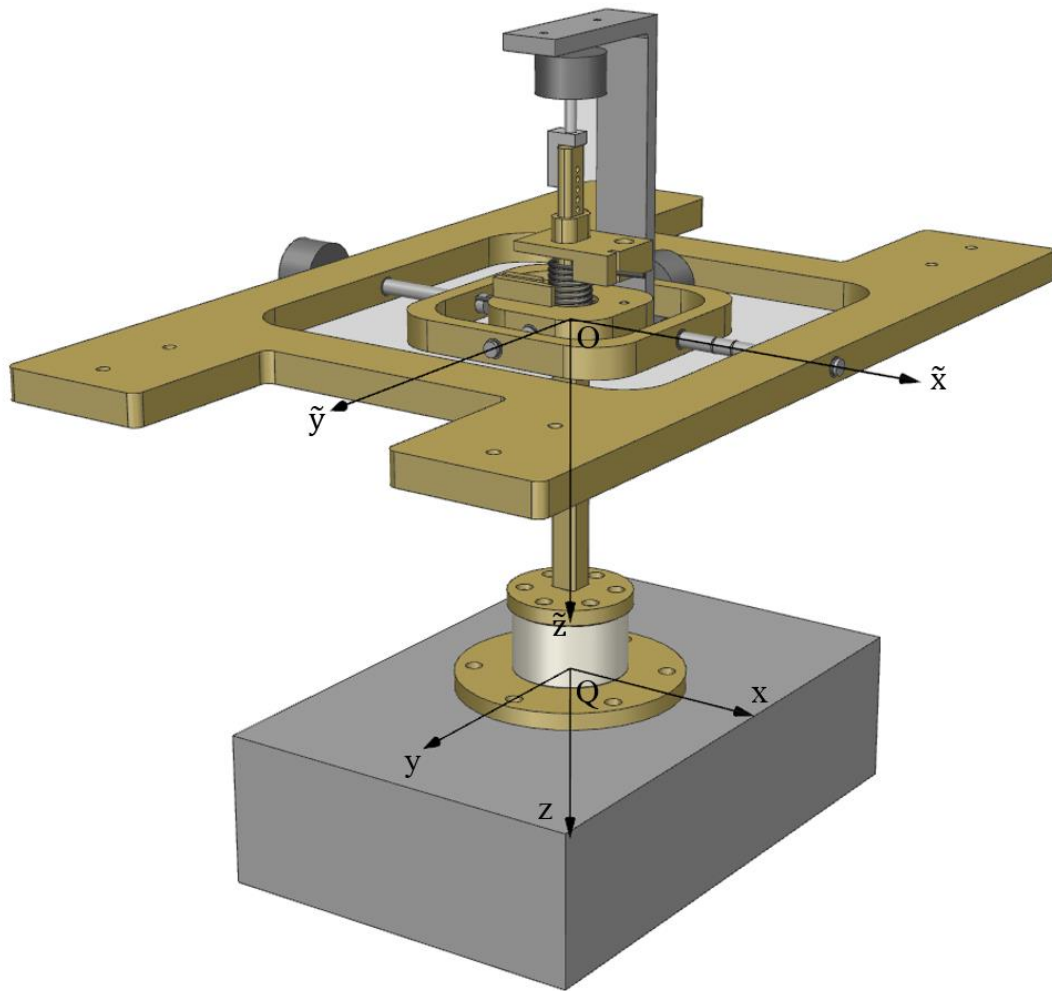
Figure 26. Computer model of **c**onfiguration of the developed design is shown.

3.1.2. Components

The testing device mainly consists of the numbered items in Figure 25. These items are:

(1) Mounting platform

(2) Nested frames

(3) Torsional Spring

(4) Extension Link

(5) Connection Interfaces

(6) Encoders

(7) Load Sensor

(8) Test Specimen

(9) Data Acquisition Systems (not shown in Figure 25)

<u>Mounting Platform</u>

Mounting platform is the main frame which carries all the parts of the test device. 90x90 mm and 45x90 mm aluminum shapes are used to construct the mounting platform. Its general look is shown in Figure 27. Maximum dimensions of a body to be mounted can be 500×500×500 mm.
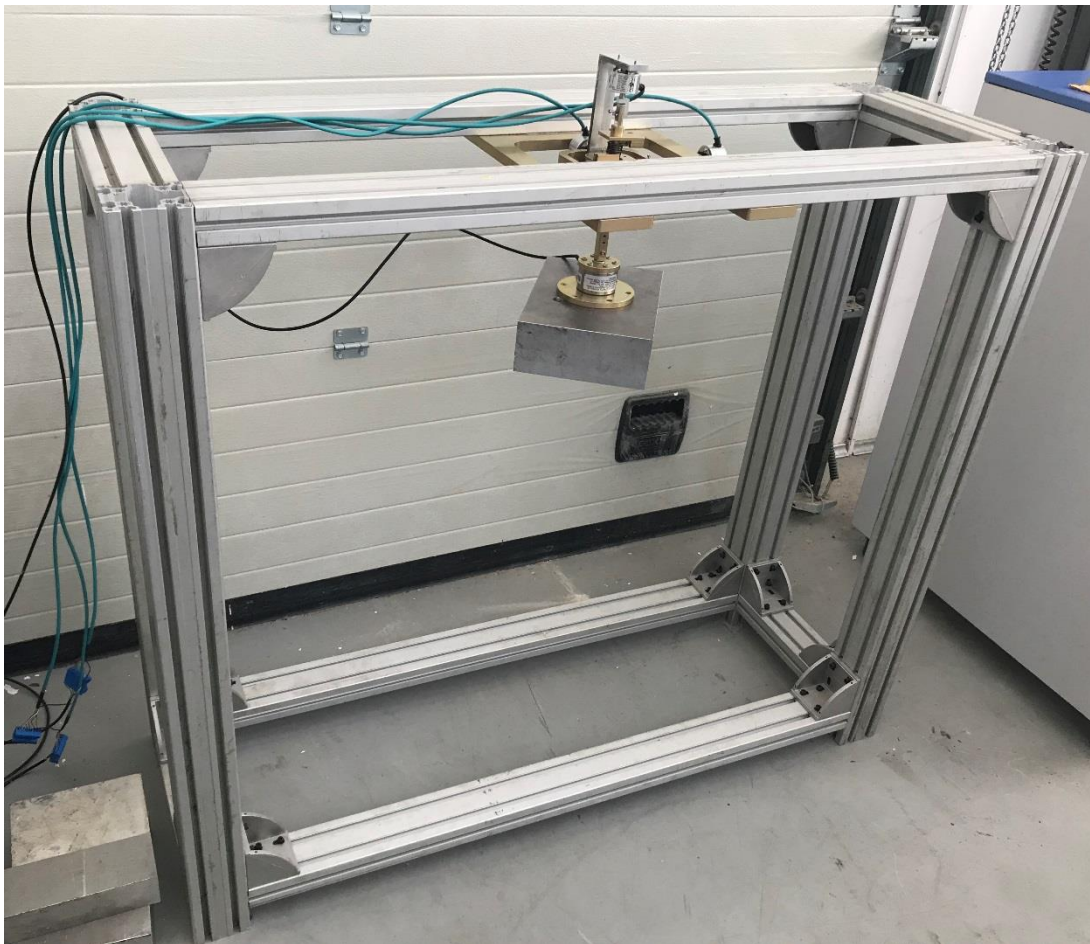
Figure 27. Mounting platform with the connected parts is shown.

<u>Nested Frames</u>

Nested frames are connected to each other with pins whose axes intersect at point O as shown in Figure 28. Using the shown pin configuration, frame 1 is able to rotate about x axis with respect to frame 2, and frame 2 is able to rotate about y axis with respect to frame 3.
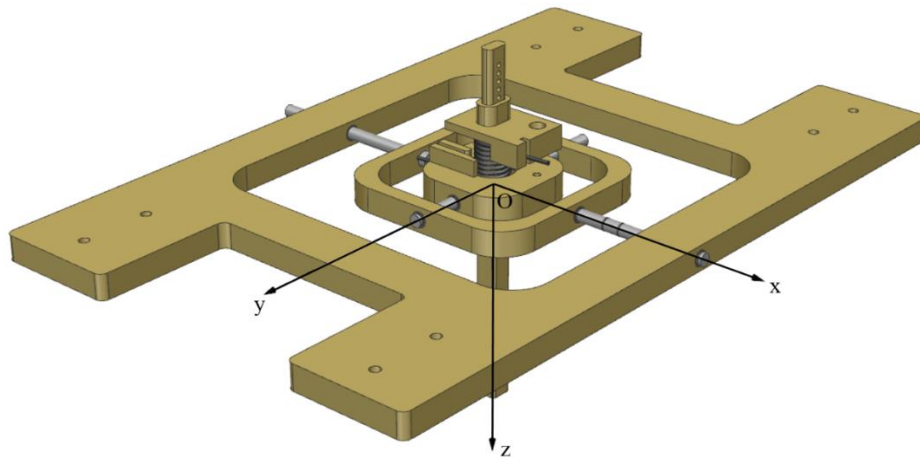
Figure 28. Nested frames and the reference coordinate axes are shown.

There is an angular contact ball bearing inside the frame 1 as shown in figure. This bearing links the frame 1 and extension link and it only allows the rotation about z axis between frame 1 and extension link. Section view is shown in Figure 29.
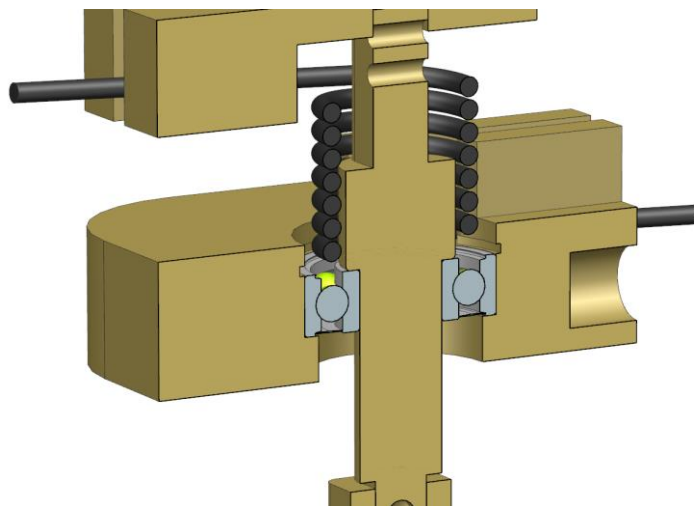
Figure 29. Bearing and rotational spring between the frame 1 and the extension link is shown.

Extension Link

Extension link shown in Figure 30 is the part which carries the rotational motion to the body to be tested. It is designed in two pieces in order to ease placing it to frame 1. At the upper side of extension link, there is a part fixes one end of torsional spring to the extension link. At lower side, there is the connection interface to the load sensor.

The length of the extension link decides the span of the testing field and period of oscillatory rotational motions about x and y axes.
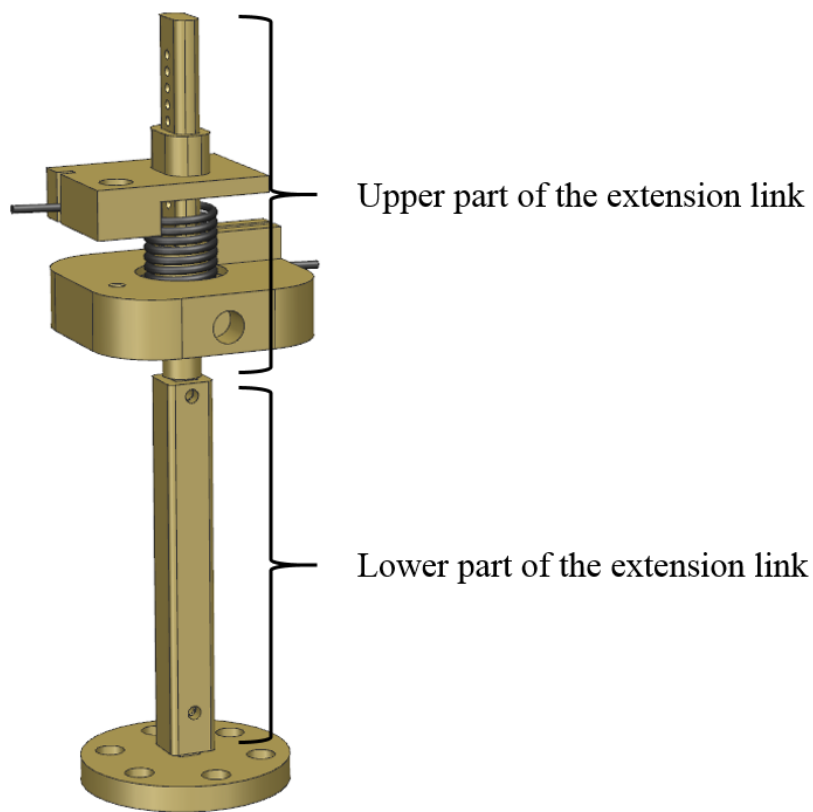
Figure 30. Extension link and connected parts are shown.

Torsional Spring

Torsional spring is placed between frame 1 and extension link as shown in Figure 31. It induces an oscillatory rotational motion between frame 1 and extension link along z axis.

The rate of the spring specifies the period of oscillatory motion about z axis.
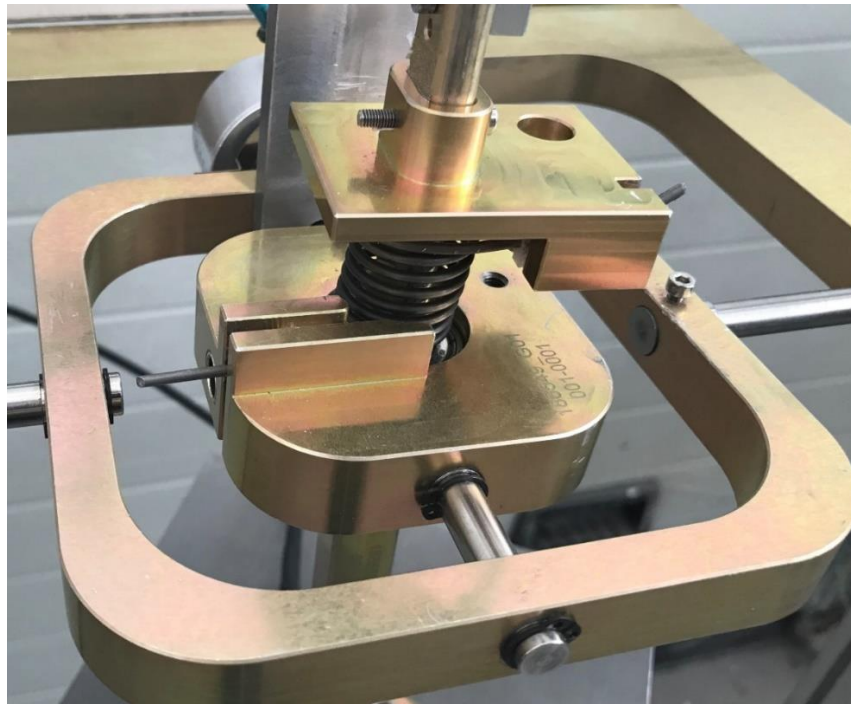
Figure 31. Torsional spring between frame 1 and extension link

Rotary Encoders

Three rotary encoders shown in Figure 32 are used in the test setup. They are recording the rotational motion between nested frames and extension link. Therefore, angular velocities and accelerations of the test specimen about point O can be obtained.

Figure 32. Encoder and connection to the frame is shown.

Encoders are incremental type. That means their first recordings start with zero value each time the power is supplied to them. Therefore, before powering up the encoders, they should be brought into the reference position.

Specifications of the encoders are given in Appendix A.

Load Sensor

Since the forces and moments should be known to use in equations of motion in all directions, six axis load sensor shown in Figure 33 is used in the test setup. The load sensor is able to measure three force values along x, y, z axes and three moment values about x, y, z axes at point Q.

Figure 33. 6-axis load sensor and its connection interfaces

Load sensor is used with an amplifier. Specifications of the load sensor and amplifier are given in Appendix B.

Data Acquisition System

Encoders and load sensor do not give physical outputs directly. Therefore, data acquisition systems are used to convert outputs of the encoders and load sensor into

physical quantities like position vs time or load vs time graphics via computers. Two different data acquisition systems are used in the device and shown in the Figure 34.

Figure 34. Data acquisition systems for load sensor and encoders

3.2. THEORY

The main requirement of the test device is to obtain all the mass parameters in a single configuration; i.e., without having to reassemble the test setup. For this purpose, three-dimensional rotational motion is governed.

As in concepts in the literature, the main consideration of the design is to provide a rotational motion in three-dimension to specimen to be tested, and measure its kinematic and kinetic quantities. In order to fulfil these requirements, the setup in the Figure 26 is designed.

The test specimen and the load sensor are rigidly attached to the extension link so that they move all together. The test specimen is able to rotate about point O under favor of attachment configurations of extension link and nested frames.

Assuming the coordinate frame located at point O which is shown in Figure 26 is attached to the extension link and moves with it, it can be inferred that the extension link can rotate about only z axis relative to frame 1. Pin connection between frame 1 and frame 2 allows rotational motion about y axis relative to each other. Similarly, frame 2 can rotate about x axis with respect to frame 3 with the pin connections shown. Superimposing these three rotational motions enables the rotation of the test specimen about point O.

If an initial motion is supplied to the test specimen, it starts to rotate about point O. The rotations about x and y axes are oscillatory motions due to the restoring effect of weight of the test specimen. Therefore, non-zero moment values about these axes can be obtained. However, rotation about z axis slows down with a low acceleration value without an oscillation, and low acceleration value means low moment measurement about z axis. Low moment measurements are more sensitive to measurement errors. Hence, the rotational spring is attached between extension link and frame 1 as shown in figure. By doing this, if sufficient initial rotation about z axis is also given to the test specimen, it starts to oscillate also about the z axis and higher moment values can be measured.

Force and moment values occurred due to motion of the body is measured by the six-axis load sensor located at point Q. Therefore, force and moment vectors affecting the body (F_Q and M_Q) are known at point Q.

Since forces and moments are known at point Q, equations (2.50) can also be written at point Q as follows

$$\begin{Bmatrix} \Sigma F_x \\ \Sigma F_y \\ \Sigma F_z \end{Bmatrix} = m \left(\begin{Bmatrix} a_{Qx} + g_x \\ a_{Qy} + g_y \\ a_{Qz} + g_z \end{Bmatrix} + \begin{bmatrix} -\omega_y^2 - \omega_z^2 & -\alpha_z + \omega_x \omega_y & \alpha_y + \omega_x \omega_z \\ \alpha_z + \omega_x \omega_y & -\omega_x^2 - \omega_z^2 & -\alpha_x + \omega_y \omega_z \\ -\alpha_y + \omega_x \omega_z & \alpha_x + \omega_y \omega_z & -\omega_x^2 - \omega_y^2 \end{bmatrix} \begin{Bmatrix} x \\ y \\ z \end{Bmatrix} \right),$$

$$\begin{Bmatrix} \Sigma M_x \\ \Sigma M_y \\ \Sigma M_z \end{Bmatrix} = m \begin{bmatrix} 0 & a_{Qz} + g_z & -a_{Qy} - g_y \\ -a_{Qz} - g_z & 0 & a_{Qx} + g_x \\ a_{Qy} + g_y & -a_{Qx} - g_x & 0 \end{bmatrix} \begin{Bmatrix} x \\ y \\ z \end{Bmatrix} + \begin{bmatrix} I_{xx} & I_{xy} & I_{xz} \\ I_{xy} & I_{yy} & I_{yz} \\ I_{xz} & I_{yz} & I_{zz} \end{bmatrix} \begin{Bmatrix} \alpha_x \\ \alpha_y \\ \alpha_z \end{Bmatrix}$$

$$+ \begin{bmatrix} 0 & -\omega_z & \omega_y \\ \omega_z & 0 & -\omega_x \\ -\omega_y & \omega_x & 0 \end{bmatrix} \begin{bmatrix} I_{xx} & I_{xy} & I_{xz} \\ I_{xy} & I_{yy} & I_{yz} \\ I_{xz} & I_{yz} & I_{zz} \end{bmatrix} \begin{Bmatrix} \omega_x \\ \omega_y \\ \omega_z \end{Bmatrix}.$$

$$(3.1)$$

Figure 35. Sequential rotation and intermediate coordinate systems are demonstrated

Rotational velocity and acceleration values seen in equations (3.1) are derived using the outputs of the encoders. Taking derivatives of these angular displacements does not give the rotational velocity of the body directly. Because the measured angular displacements are the rotations of the intermediate coordinate systems between the fixed and body coordinate systems. Using Figure 35, that statement can be explained more precisely as

- θ_1 is the relative displacement about x axis between the fixed coordinate system attached to the nested frame 1 (XYZ) and the first intermediate coordinate system attached to the nested frame 2 ($x'y'z'$),

- θ_2 is the relative displacement about y axis between the first intermediate coordinate system attached to the nested frame 2 ($x'y'z'$) and the second intermediate coordinate system attached to the nested frame 3 ($x''y''z''$),
- θ_3 is the relative displacement about z axis between the fixed coordinate system attached to the nested frame 3 ($x''y''z''$) and local coordinate system attached to extension link and therefore to the test specimen (xyz).

These angular displacements are called as 'Euler's Angles' which are demonstrated in Figure 35. For the configuration of frames used in the test setup, rotation about x axis (θ_1) is applied first, because the motion of the test setup starts with the rotation about x axis between the fixed coordinate system the first intermediate coordinate system. Then, rotations about y and z axes (θ_2 and θ_3) are applied respectively with the similar sense. These sequenced rotations can be named as '1-2-3 Euler Rotation Sequence'. Further information about Euler's angles and rotation sequences are in Appendix C.

Since the measured Euler's angles in the test setup are obtained with respect to different coordinate systems, in order to find the angular velocity of the body, derivatives of the measured rotations should be transformed to the body-fixed coordinate system. Then, taking the derivative of angular velocity gives the angular acceleration. Equations to calculate angular velocity and acceleration are given in 3.2. Detailed procedure to obtain these equations are also given in Appendix C

$$\boldsymbol{\omega} = \begin{Bmatrix} \omega_x \\ \omega_y \\ \omega_z \end{Bmatrix} = \begin{bmatrix} \cos\theta_1 \cos\theta_3 & \sin\theta_3 & 0 \\ -\cos\theta_1 \sin\theta_3 & \cos\theta_3 & 0 \\ \sin\theta_1 & 0 & 1 \end{bmatrix} \begin{Bmatrix} \dot\theta_1 \\ \dot\theta_2 \\ \dot\theta_3 \end{Bmatrix},$$

$$\boldsymbol{\alpha} = \dot{\boldsymbol{\omega}}. \tag{3.2}$$

Translational velocities and accelerations at point Q are obtained by the method given in Chapter 2.1.4 with the following equations

$$\boldsymbol{v}_Q = \boldsymbol{\omega} \times \boldsymbol{r}_Q,$$

$$\boldsymbol{a}_Q = \boldsymbol{\alpha} \times \boldsymbol{r}_Q + \boldsymbol{\omega} \times (\boldsymbol{\omega} \times \boldsymbol{r}_Q). \tag{3.3}$$

These force, moment, velocity and acceleration measurements are done continuously during the motion of the specimen. Therefore, for every time instant, there are force, moment, velocity and acceleration values for point Q.

3.2.1. Mass Measurement

It can be assumed that there are two different coordinate systems located at point O. One of them is the fixed reference coordinate system (global frame, $\tilde{x}\tilde{y}\tilde{z}$) and the other one is the rotating coordinate system (local frame, xyz) which is moving with the test specimen.

Firstly, the axes of reference and local coordinate systems should be coincident at the starting of the test. That is the reference position for the encoders, and the position measurements start relative to that non-rotated position.

Then the test setup should be released and come into the static equilibrium position. In the static equilibrium position, the test specimen is going to be in an inclined position if the center of gravity does not coincide with the vertical axis passing through point O.

In that static equilibrium position, equation $(3.1)_a$ can be simplified as follows

$$\begin{Bmatrix} \Sigma F_{Qx} \\ \Sigma F_{Qy} \\ \Sigma F_{Qz} \end{Bmatrix} = m \begin{Bmatrix} g_x \\ g_y \\ g_z \end{Bmatrix}. \tag{3.4}$$

where $\{g\} = [g_x \quad g_y \quad g_z]^T$ is the gravitational acceleration components in local frame and $\Sigma F = [\Sigma F_{Qx} \quad \Sigma F_{Qy} \quad \Sigma F_{Qz}]^T$ is the force measurements of load sensor.

The $\{g\}$ vector is obtained by a transformation matrix between reference and local coordinate system as follows

$$\{g\} = [T]\{\tilde{g}\}. \tag{3.5}$$

where $[\boldsymbol{T}]$ is the transformation matrix, $\{\tilde{\boldsymbol{g}}\}$ is the gravitational accelerations in global frame. Gravitational accelerations in global frame, $\{\tilde{\boldsymbol{g}}\}$, can directly be written as

$$\{\tilde{\boldsymbol{g}}\} = \begin{Bmatrix} \tilde{g}_x \\ \tilde{g}_y \\ \tilde{g}_z \end{Bmatrix} = \begin{Bmatrix} 0 \\ 0 \\ g_0 \end{Bmatrix}. \tag{3.6}$$

where g_0 is the standard gravity and equals to 9.80665 m/s^2 [68].

Transformation matrix can be derived by using Euler rotations in xyz sequence. Then the transformation matrix, $[\boldsymbol{T}]$, in equation (3.5) can be rewritten as

$$[\boldsymbol{T}] = \begin{bmatrix} \cos\theta_2 \cos\theta_3 & \cos\theta_1 \sin\theta_3 + \sin\theta_1 \sin\theta_2 \cos\theta_3 & \sin\theta_1 \sin\theta_3 - \cos\theta_1 \sin\theta_2 \cos\theta_3 \\ -\cos\theta_2 \sin\theta_3 & \cos\theta_1 \cos\theta_3 - \sin\theta_1 \sin\theta_2 \sin\theta_3 & \sin\theta_1 \cos\theta_3 + \cos\theta_1 \sin\theta_2 \sin\theta_3 \\ \sin\theta_2 & -\sin\theta_1 \cos\theta_2 & \cos\theta_1 \cos\theta_2 \end{bmatrix}.$$

$$\tag{3.7}$$

where θ_1, θ_2 and θ_3 are Euler angles which are the angular positions about x, y and z axes relatively. These angular positions are the recordings of the encoders at the static equilibrium position.

Coordinate transformation for force and moment measurements are not required since the load sensor is moving with the local coordinate frame, its measurements can directly be used in equations of motion.

If the components of gravitational acceleration in local frame and the force measurements of load sensor are replaced into equation (3.4), total mass of the test specimen can be calculated. Then, mass of the test specimen, m, is calculated as follows

$$m = \frac{F_x}{g_x},$$

$$m = \frac{F_y}{g_y},$$ (3.8)

$$m = \frac{F_z}{g_z}.$$

Theoretically, for each equality in equation (3.8) should give the same result; however, due to the inaccuracies in the test configuration and measurement errors, the results differ a little. Therefore, average of these measurements is taken as a result as

$$m = \frac{\frac{F_x}{g_x} + \frac{F_y}{g_y} + \frac{F_z}{g_z}}{3}.$$ (3.9)

3.2.2. Center of Gravity Measurement

After the mass of the test specimen is calculated in static position, center of gravity of the test specimen can also be measured in the same position. For the center of gravity position, rotational equation of motion equation $(3.1)_b$ is used. In the static equilibrium position, equation $(3.1)_b$ gets in the following form

$$\begin{Bmatrix} \Sigma M_{Qx} \\ \Sigma M_{Qy} \\ \Sigma M_{Qz} \end{Bmatrix} = m \begin{bmatrix} 0 & g_z & -g_y \\ -g_z & 0 & g_x \\ g_y & -g_x & 0 \end{bmatrix} \begin{Bmatrix} x \\ y \\ z \end{Bmatrix}.$$ (3.10)

where $\Sigma \boldsymbol{M} = [\Sigma M_{Qx} \quad \Sigma M_{Qy} \quad \Sigma M_{Qz}]^T$ is the moment measurements of the load sensor and $[x \quad y \quad z]^T = \boldsymbol{r}_G$ is the center of gravity position of the test specimen relative to the local coordinate system.

Solution of the equation (3.10) gives the center of gravity position $\boldsymbol{r}_G$.

Calculated center of gravity position of the test specimen, $\boldsymbol{r}_G$, is relative to the measurement point Q. Center of gravity of the specimen can also be written with respect to the local coordinate frame whose origin is at point O as follows

$$r_{G/O} = r_Q + r_G. \tag{3.11}$$

where r_Q is the position vector of point Q in the local frame located at point O.

It is also possible to obtain center of gravity positions in a dynamical test. After the mass is measured and the encoders are still in recording, an initial rotational displacement about all three axes of the local frame are given to the test specimen. The specimen starts to make an oscillatory motion about these axes. While the test specimen is making and oscillatory motion, load sensor and encoders are recording loads and positions continuously. Therefore, at point Q, there are force and moment measurements from the load sensor, and position, velocity and acceleration measurements from the encoders for every time instant.

Using equation $(3.1)_1$, three equations can be written with the measurements for a single time instant. By constituting three equations for every time instant, the following over-constrained system is obtained

$$\begin{Bmatrix} \Sigma F_{Qx_1} \\ \Sigma F_{Qy_1} \\ \Sigma F_{Qz_1} \\ \vdots \\ \vdots \\ \Sigma F_{Qx_n} \\ \Sigma F_{Qy_n} \\ \Sigma F_{Qz_n} \end{Bmatrix}_{3n\times 1} - m \begin{Bmatrix} a_{Qx_1} + g_{x_1} \\ a_{Qy_1} + g_{y_1} \\ a_{Qz_1} + g_{z_1} \\ \vdots \\ \vdots \\ a_{Qx_n} + g_{x_n} \\ a_{Qy_n} + g_{y_n} \\ a_{Qz_n} + g_{z_n} \end{Bmatrix}_{3n\times 1}$$

$$= \begin{bmatrix} -\omega_{y_1}^2 - \omega_{z_1}^2 & -\alpha_{z_1} + \omega_{x_1}\omega_{y_1} & \alpha_{y_1} + \omega_{x_1}\omega_{z_1} \\ \alpha_{z_1} + \omega_{x_1}\omega_{y_1} & -\omega_{x_1}^2 - \omega_{z_1}^2 & -\alpha_{x_1} + \omega_{y_1}\omega_{z_1} \\ -\alpha_{y_1} + \omega_{x_1}\omega_{z_1} & \alpha_{x_1} + \omega_{y_1}\omega_{z_1} & -\omega_{x_1}^2 - \omega_{y_1}^2 \\ & \vdots & \\ & \vdots & \\ -\omega_{y_n}^2 - \omega_{z_n}^2 & -\alpha_{z_n} + \omega_{x_n}\omega_{y_n} & \alpha_{y_n} + \omega_{x_n}\omega_{z_n} \\ \alpha_{z_n} + \omega_{x_n}\omega_{y_n} & -\omega_{x_n}^2 - \omega_{z_n}^2 & -\alpha_{x_n} + \omega_{y_n}\omega_{z_n} \\ -\alpha_{y_n} + \omega_{x_n}\omega_{z_n} & \alpha_{x_n} + \omega_{y_n}\omega_{z_n} & -\omega_{x_n}^2 - \omega_{y_n}^2 \end{bmatrix}_{3n\times 3} \begin{Bmatrix} x \\ y \\ z \end{Bmatrix}.$$

$$\tag{3.12}$$

For a more compact view, equation (3.12) can be rewritten as follows

$$\{A_1\}_{3n\times 1} = [A_2]_{3n\times 3}\{r_G\}, \tag{3.13}$$

where

$$\{A_1\}_{3n\times 1} = \begin{Bmatrix} \Sigma F_{Qx_1} \\ \Sigma F_{Qy_1} \\ \Sigma F_{Qz_1} \\ \vdots \\ \vdots \\ \Sigma F_{Qx_n} \\ \Sigma F_{Qy_n} \\ \Sigma F_{Qz_n} \end{Bmatrix}_{3n\times 1} - m \begin{Bmatrix} a_{Qx_1} + g_{x_1} \\ a_{Qy_1} + g_{y_1} \\ a_{Qz_1} + g_{z_1} \\ \vdots \\ \vdots \\ a_{Qx_n} + g_{x_n} \\ a_{Qy_n} + g_{y_n} \\ a_{Qz_n} + g_{z_n} \end{Bmatrix}_{3n\times 1} ,$$

$$[A_2]_{3n\times 3} = \begin{bmatrix} -\omega_{y_1}^2 - \omega_{z_1}^2 & -\alpha_{z_1} + \omega_{x_1}\omega_{y_1} & \alpha_{y_1} + \omega_{x_1}\omega_{z_1} \\ \alpha_{z_1} + \omega_{x_1}\omega_{y_1} & -\omega_{x_1}^2 - \omega_{z_1}^2 & -\alpha_{x_1} + \omega_{y_1}\omega_{z_1} \\ -\alpha_{y_1} + \omega_{x_1}\omega_{z_1} & \alpha_{x_1} + \omega_{y_1}\omega_{z_1} & -\omega_{x_1}^2 - \omega_{y_1}^2 \\ & \vdots & \\ & \vdots & \\ -\omega_{y_n}^2 - \omega_{z_n}^2 & -\alpha_{z_n} + \omega_{x_n}\omega_{y_n} & \alpha_{y_n} + \omega_{x_n}\omega_{z_n} \\ \alpha_{z_n} + \omega_{x_n}\omega_{y_n} & -\omega_{x_n}^2 - \omega_{z_n}^2 & -\alpha_{x_n} + \omega_{y_n}\omega_{z_n} \\ -\alpha_{y_n} + \omega_{x_n}\omega_{z_n} & \alpha_{x_n} + \omega_{y_n}\omega_{z_n} & -\omega_{x_n}^2 - \omega_{y_n}^2 \end{bmatrix}_{3n\times 3} .$$

The over-constrained system can be solved by the least-square method with the following equation [69], [70]

$$r_G = ([A_2]^T [A_2])^{-1} [A_2]^T \{A_1\}. \tag{3.14}$$

3.2.3. Inertia Measurement

Inertia parameters of the test specimen are determined in a dynamical test. They can be calculated either after the center of gravity position is determined or concurrently with center of gravity position.

Inertia parameters are calculated using both translational and rotational equations of motion. Equation $(3.1)_1$ and $(3.1)_2$ can be combined by creating unknowns vector including center of gravity locations and inertia parameters as follows

$$\begin{Bmatrix} \Sigma F_Q - m\{a_Q + g\} \\ \Sigma M_Q \end{Bmatrix} = \begin{bmatrix} m[A_3] & [0] \\ m[A_4] & [A_5] \end{bmatrix} \begin{Bmatrix} r_G \\ I_Q \end{Bmatrix}, \qquad (3.15)$$

where $r_G = [x \quad y \quad z]^T$ and $I_Q = [I_{xx} \quad I_{yy} \quad I_{zz} \quad I_{xy} \quad I_{xz} \quad I_{yz}]^T$ is the inertia parameters of the test specimen.

$$[A_3] = \begin{bmatrix} -\omega_y^2 - \omega_z^2 & -\alpha_z + \omega_x\omega_y & \alpha_y + \omega_x\omega_z \\ \alpha_z + \omega_x\omega_y & -\omega_x^2 - \omega_z^2 & -\alpha_x + \omega_y\omega_z \\ -\alpha_y + \omega_x\omega_z & \alpha_x + \omega_y\omega_z & -\omega_x^2 - \omega_y^2 \end{bmatrix},$$

$$[A_4] = \begin{bmatrix} 0 & a_{Qz} + g_z & -a_{Qy} - g_y \\ -a_{Qz} - g_z & 0 & a_{Qx} + g_x \\ a_{Qy} + g_y & -a_{Qx} - g_x & 0 \end{bmatrix},$$

$$[A_5] = \begin{bmatrix} \alpha_x & -\omega_y\omega_z & \omega_y\omega_z & \alpha_y - \omega_x\omega_z & \alpha_z + \omega_x\omega_y & \omega_y^2 - \omega_z^2 \\ \omega_x\omega_z & \alpha_y & -\omega_x\omega_z & \alpha_x + \omega_y\omega_z & \omega_z^2 - \omega_x^2 & \alpha_z - \omega_x\omega_y \\ -\omega_x\omega_y & \omega_x\omega_y & \alpha_z & \omega_x^2 - \omega_y^2 & \alpha_x - \omega_y\omega_z & \alpha_y + \omega_x\omega_z \end{bmatrix}.$$

Equation 3.15 can be shown in a more compact form as follows

$$\{A_6\} = [A_7]\{X\}, \qquad (3.16)$$

where $\{X\} = [x \quad y \quad z \quad I_{xx} \quad I_{yy} \quad I_{zz} \quad I_{xy} \quad I_{xz} \quad I_{yz}]^T$,

$$\{A_6\} = \begin{Bmatrix} \Sigma F_Q - m\{a_Q + g\} \\ \Sigma M_Q \end{Bmatrix},$$

$$[A_7] = \begin{bmatrix} m[A_3] & [0] \\ m[A_4] & [A_5] \end{bmatrix}.$$

Equation (3.16) can also be constructed for every time instant for different force, moment, velocity and acceleration measurement values and the following over-constrained system can be obtained

$$\begin{Bmatrix} A_{6_1} \\ \vdots \\ A_{6_n} \end{Bmatrix}_{6n \times 1} = \begin{bmatrix} A_{7_1} \\ \vdots \\ A_{7_n} \end{bmatrix}_{6n \times 9} \{X\}_{9 \times 1}. \tag{3.17}$$

That over-constrained system can also be shown in more compact form as

$$\{A_8\}_{6n \times 1} = [A_9]_{6n \times 9} \{X\}_{9 \times 1}, \tag{3.18}$$

where $\{A_8\}_{6n \times 1} = \begin{Bmatrix} A_{6_1} \\ \vdots \\ A_{6_n} \end{Bmatrix}_{6n \times 1}$, $[A_9]_{6n \times 9} = \begin{bmatrix} A_{7_1} \\ \vdots \\ A_{7_n} \end{bmatrix}_{6n \times 9}$.

Then, the unknown matrix $\{X\}$, which contains center of gravity positions and inertia parameters, can be solved by a least square method as follows

$$\{X\} = ([A_9]^T [A_9])^{-1} [A_9]^T \{A_8\}, \tag{3.19}$$

First three terms of the unknown matrix $\{X\}$ gives r_Q vector, and the last six terms gives I_Q vector.

Inertia parameters calculated in I_Q vector are about the local coordinate system at point Q. The inertia parameters about the center of gravity locations can be obtained using parallel axis theorem as in equation (2.51)

$$[I_G] = [I_Q] - m \begin{bmatrix} y^2 + z^2 & -xy & -xz \\ -xy & x^2 + z^2 & -yz \\ -xz & -yz & x^2 + y^2 \end{bmatrix}. \tag{3.20}$$

where x, y, z are the elements of the center of gravity position vector of the test specimen relative to point Q, $r_G = [x \quad y \quad z]^T$.

Alternatively, if mass and center of gravity positions are found previously, rotational equations of motion can be used to obtain inertia parameters of the test specimen about the center of gravity location directly. In order to do this, rotational equations of motion

should be written at center of gravity point, G. If the forces and moments at point Q are translated to point G, the following is obtained

$$
\begin{aligned}
\boldsymbol{F}_G &= \boldsymbol{F}_Q, \\
\boldsymbol{M}_G &= \boldsymbol{M}_Q + \boldsymbol{r}_G \times \boldsymbol{F}_Q.
\end{aligned}
\tag{3.21}
$$

Then, rotational equation of motion can be rewritten in the following form

$$
\{\boldsymbol{M}_G\} = \begin{bmatrix}
\alpha_x & -\omega_y\omega_z & \omega_y\omega_z & \alpha_y - \omega_x\omega_z & \alpha_z + \omega_x\omega_y & \omega_y^2 - \omega_z^2 \\
\omega_x\omega_z & \alpha_y & -\omega_x\omega_z & \alpha_x + \omega_y\omega_z & \omega_z^2 - \omega_x^2 & \alpha_z - \omega_x\omega_y \\
-\omega_x\omega_y & \omega_x\omega_y & \alpha_z & \omega_x^2 - \omega_y^2 & \alpha_x - \omega_y\omega_z & \alpha_y + \omega_x\omega_z
\end{bmatrix} \{\boldsymbol{I}_G\},
$$

$$
\{\boldsymbol{M}_G\} = [\boldsymbol{A}_5]\,\{\boldsymbol{I}_G\}.
\tag{3.22}
$$

where $\boldsymbol{I}_G$ is inertia parameters of test specimen about point G.

In this instance, if equation $\{\boldsymbol{M}_G\} = [\boldsymbol{A}_5]\,\{\boldsymbol{I}_G\}$ is written for every time instant, over-constrained system can be written as follows

$$
\begin{Bmatrix} \boldsymbol{M}_{G_1} \\ \vdots \\ \boldsymbol{M}_{G_n} \end{Bmatrix}_{3n\times1} = \begin{bmatrix} \boldsymbol{A}_{5_1} \\ \vdots \\ \boldsymbol{A}_{5_n} \end{bmatrix}_{3n\times6} \{\boldsymbol{I}_G\}_{6\times1},
\tag{3.23}
$$

or in a more compact form as

$$
\{\boldsymbol{A}_{10}\}_{3n\times1} = [\boldsymbol{A}_{11}]_{3n\times6}\,\{\boldsymbol{I}_G\}_{6\times1},
\tag{3.24}
$$

where $\{\boldsymbol{A}_{10}\}_{3n\times1} = \begin{Bmatrix} \boldsymbol{M}_{G_1} \\ \vdots \\ \boldsymbol{M}_{G_n} \end{Bmatrix}_{3n\times1}$, $[\boldsymbol{A}_{11}]_{3n\times6} = \begin{bmatrix} \boldsymbol{A}_{5_1} \\ \vdots \\ \boldsymbol{A}_{5_n} \end{bmatrix}_{3n\times6}$.

Then, the inertia parameters about center of gravity position, $\boldsymbol{I}_G$, can be directly found by solving the following equation,

$$
\boldsymbol{I}_G = ([\boldsymbol{A}_{11}]^T\,[\boldsymbol{A}_{11}])^{-1}\,[\boldsymbol{A}_{11}]^T\,\{\boldsymbol{A}_{10}\}.
\tag{3.25}
$$

CHAPTER 4

SAMPLE SIMULATION, TESTS AND RESULTS

In that part of the thesis, the method of measuring the mass properties explained in Chapter 3 is applied for different cases. Firstly, a computer simulation model is constructed by using MSC Adams software and the measurement methods are applied. Then, mass properties of some dummy masses are calculated using the real test setup. The results of the computer simulation and the real tests are compared to the real values of the mass properties of the test specimens.

4.1. CASE I – COMPUTER SIMULATION

The same test configuration developed in the Chapter 3 is modeled by using MSC Adams software. An arbitrary shape solid model is used for calculation of the mass properties.

Rotational motion in three-dimension is given to the specimen which is demonstrated in the Figure 36.
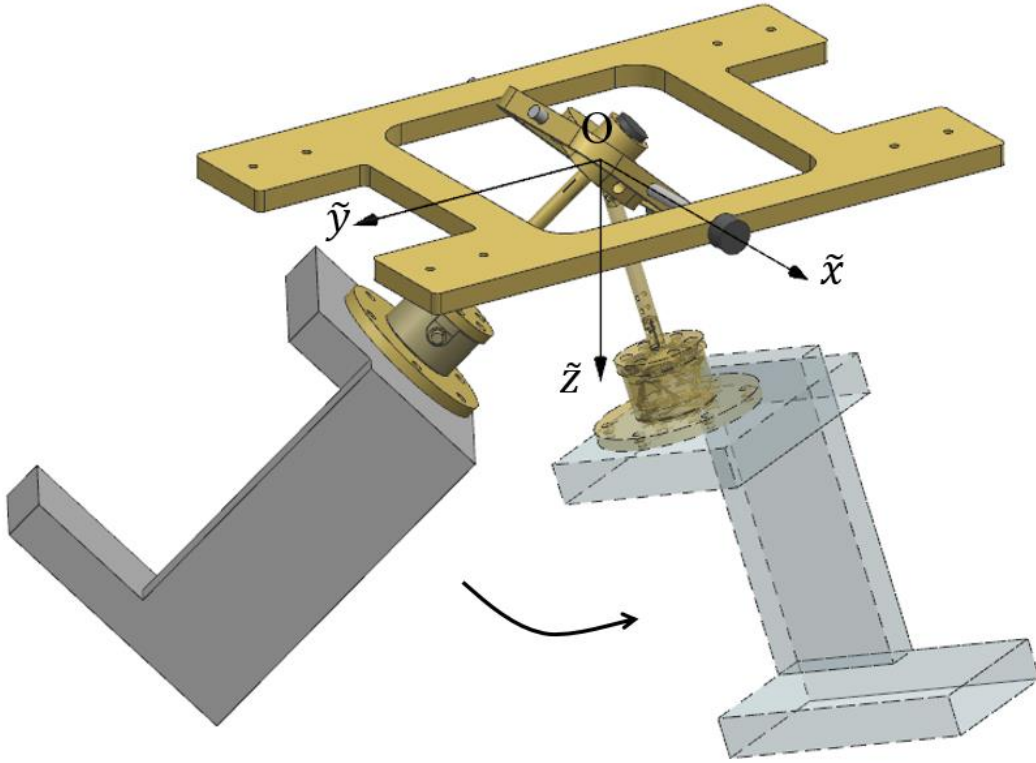
Figure 36. The arbitrary shape solid model is demonstrated.

Test specimen can make a rotational motion about point O. The specimen is brought to the initial position by using an Euler's rotation angles $-42°, -17°, 120°$ about x, y, z axes, respectively.

When the simulation starts, the specimen makes an oscillatory rotational motion about point O. During the motion, Euler's angles $(\theta_1, \theta_2, \theta_3)$, force and moment values at point Q ($\Sigma F_{Qx}, \Sigma F_{Qy}, \Sigma F_{Qz}, \Sigma M_{Qx}, \Sigma M_{Qy}, \Sigma M_{Qz}$) are measured.

4.1.1. Mass Measurement

The mass measurement method explained in Chapter 3.2.1 is applied. At the time when the simulation starts, the force values at the load cell in local coordinate frame is measured as follows

$$\begin{Bmatrix} F_{Qx,0} \\ F_{Qy,0} \\ F_{Qz,0} \end{Bmatrix} = \begin{Bmatrix} 104.9 \\ -21.75 \\ -109.3 \end{Bmatrix} N.$$

Then, the transformation matrix at the initial position is formed by using the equation (3.7) as follows

$$[T] = \begin{bmatrix} -0.4870 & 0.5669 & 0.5669 \\ -0.8258 & -0.5465 & 0.1390 \\ -0.2843 & 0.6164 & 0.7343 \end{bmatrix}.$$

Gravitational acceleration components in the local frame is obtained by equation (3.5)

$$\{g_0\} = \begin{Bmatrix} g_{x,0} \\ g_{y,0} \\ g_{z,0} \end{Bmatrix} = \begin{Bmatrix} 6.7230 \\ -1.3825 \\ -7.0043 \end{Bmatrix} m/s^2.$$

Mass of the test specimen is calculated by using equations (3.8) and (3.9). The result of the mass measurement is the following

$$m = 15.6 \; kg.$$

The mass measurement in computer simulation gives the exact result. The accuracy of the mass measurement is very high in the simulation model, because the force measurements are perfectly done and initial position is ensured with the exact values. Also, there is no mathematical operation other than the simple multiplication for calculating the mass of the test specimen.

4.1.2. Center of Gravity Measurement

The center of gravity measurement method explained in Chapter 3.2.2 is applied. Center of gravity position with respect to point Q can be measured in a dynamic test using equations (3.12) through (3.14). In order to get the equation system in equation (3.12), the simulation is run for 5 seconds and data are recorded with 200 Hz sampling rate. Therefore, equation system is constructed with 3000 equations. Solution of the equation system gives the center of gravity position of the test specimen with respect to point Q. Then, using equation (3.11), center of gravity position can be calculated with respect to point O. Results for these case are given in Table 1. In table, reference values of center of gravity are directly taken from simulation software.

Table 1. Center of gravity position measurements

	Reference value	Measured value	% Error
x (**mm**)	12,2555	12,4836	1,86
y (**mm**)	-62,8294	-62,8760	0,07
z (**mm**)	116,5809	116,5712	0,01

4.1.3. Inertia Measurement

Mass properties including center of gravity positions, moment and product of inertias are calculated using the method in Chapter 3.2.3. Equations (3.16) through (3.20) are utilized to obtain the inertia values about point Q. Then, inertia values are calculated about the center of gravity position using equation (3.20). Similar to the center of gravity measurement in Chapter 4.1.2, the simulation is run for 5 seconds with 200 Hz sampling rate. Therefore, equation system in equation (3.15) are constructed with 6000 equations and solved by least square solution method.

For the reference values of inertia parameters, definitions of the moments and products of inertia in equations (2.39) and (2.40) are used. For that purpose, the simulation model is divided into three segments as shown in Figure 37.
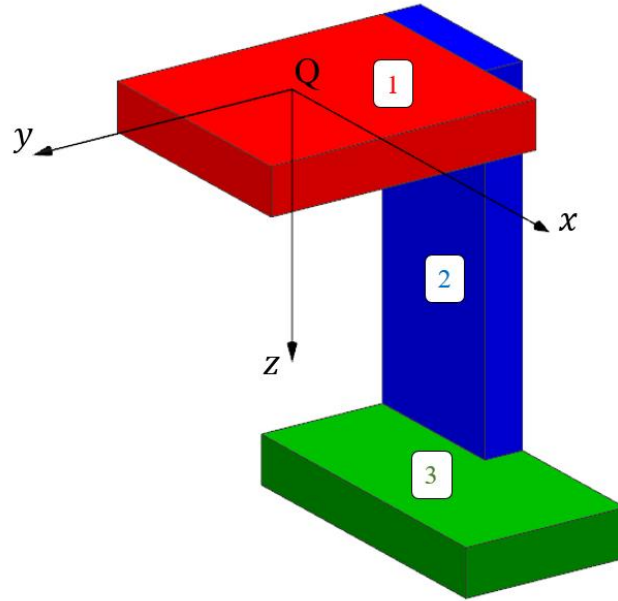
Figure 37. Arbitrary shape simulation model is divided into three segments for calculation of inertia values.

For calculation of inertia parameters of the arbitrary shape model in Figure 36, inertia values of three segments in Figure 37 are separately calculated and they are totalized. For the demonstration of the application of equations (2.39) and (2.40), moment of inertia about x axis for the segments in Figure 37 can be calculated as follows

$$I_x = \int (y^2 + z^2)\, dm = \int_{m_1} (y^2 + z^2)\, dm_1 + \int_{m_2} (y^2 + z^2)\, dm_2 + \int_{m_3} (y^2 + z^2)\, dm_3,$$

$$I_x = \int_0^{30} \int_{-103}^{73} \int_{-63}^{87} (y^2 + z^2)\, \rho\, dx_1\, dy_1\, dz_1 + \int_0^{230} \int_{-128}^{-103} \int_{-63}^{37} (y^2 + z^2)\, \rho\, dx_2\, dy_2\, dz_2$$

$$+ \int_{230}^{260} \int_{-128}^{-23} \int_{-63}^{137} (y^2 + z^2)\, \rho\, dx_1\, dy_1\, dz_1,$$

$$I_x = 486950 \; kg \cdot mm^2 = 0.48695 \; kg \cdot m^2.$$

Similar procedure can be applied to calculate the rest of the inertia parameters. The inertia parameters could also be read Adams software, directly. Calculated inertia

parameters by using the definition are exactly the same as the values directly read from the Adams software. These inertia values are used as a reference to compare the values measured by the developed design.

In Table 2, reference and measured values of center of gravity position with respect to point Q and inertia values about center of gravity are given.

Table 2. Complete mass properties measurements at point Q

	Reference value	Measured value	% Error
$x \ (mm)$	12,2555	12,2843	0,23
$y \ (mm)$	-62,8294	-62,8317	0,00
$z \ (mm)$	116,5809	116,5615	0,02
$I_x \ (kg \cdot m^2)$	0,48695	0,48696	0,00
$I_y \ (kg \cdot m^2)$	0,41775	0,41779	0,01
$I_z \ (kg \cdot m^2)$	0,14919	0,14972	0,35
$I_{xy} \ (kg \cdot m^2)$	-0,00764	-0,00791	3,46
$I_{xz} \ (kg \cdot m^2)$	0,03831	0,03915	2,20
$I_{yz} \ (kg \cdot m^2)$	-0,15159	-0,15089	0,46

Inertia measurements given in Table 2 are about point Q. Inertia measurement about center of gravity are calculated using parallel axis theorem and shown in Table 3.

Table 3. Inertia measurements about center of gravity

	Reference value	Measured value	% Error
$I_x \ (kg \cdot m^2)$	0,21329	0,21324	0,02
$I_y \ (kg \cdot m^2)$	0,20334	0,20333	0,01
$I_z \ (kg \cdot m^2)$	0,08525	0,08560	0,41
$I_{xy} \ (kg \cdot m^2)$	0,00437	0,00434	0,72
$I_{xz} \ (kg \cdot m^2)$	0,01602	0,01645	2,68
$I_{yz} \ (kg \cdot m^2)$	-0,03730	-0,03652	2,09

If the results are examined, the accuracies are said to be high. Generally, the percentage differences are lower than 0.5%. These differences are mostly caused by differentiation operation while calculating angular velocities and accelerations. If the angular velocity and acceleration values are directly taken from the computer software, instead of calculating them, all mass properties are calculated with differences less than 10^{-4} %, which are caused by the least square solution method.

4.2. CASE II – DUMMY MASS - A

The same test configuration developed in the Chapter 3 is assembled and a dummy mass shown in Figure 38 is attached as a test specimen. Dummy mass is an aluminum block with known dimensions and density. Reference mass properties are directly taken from the CAD model to compare the measured values. Since the shape of the dummy mass is simple, mass properties taken from CAD model are going to be accurate enough.

Figure 38. Shown aluminum block is used to measure mass properties.

Measuring the mass is accurate and an easy process by an ordinary weighing machine. Therefore, the mass of the test specimen (7.4 kg) is measured in advance and directly replaced into equations of motion. Then, the rest of the mass properties are measured with the test device.

As in the computer simulation case, an initial displacement is given to the test specimen. Once the rotation about point O starts, the rotation angles, force and moment values are measured with encoders and load sensor during the motion.

4.2.1. Center of Gravity Measurement

The center of gravity measurement method explained in Chapter 3.2.2 is applied. Center of gravity position with respect to point Q can be measured in a dynamic test using equations (3.12) through (3.14). In order to get the equation system in equation (3.12), Euler angles and loads are measured for 60 seconds. Solution of that equation system gives the center of gravity position of the test specimen with respect to point Q. Results for that cases are given in Table 4.

Table 4. Center of gravity position measurements for dummy mass A

	Reference value	Measured value	% Error	Standard Deviation
x (mm)	0	1.24	-	0.74
y (mm)	0	0.85	-	1.13
z (mm)	71	71.44	0.62	0.94

The results given in Table 4 are calculated using 8000 Hz data sampling rate. 5 different tests are performed with that frequency and the average of the measurements and standard deviations are given in the table. Moreover, different data sampling rates are used; however, results between these are not significant. For comparison, center of gravity measurements for different data sampling rates are given in Table 5.

Table 5. Center of gravity position measurements for different sampling rates for dummy mass A

	Reference Value	Measured values				
		100 Hz	**500 Hz**	**1000 Hz**	**4000 Hz**	**8000 Hz**
x (mm)	0	1.12	1.27	2.59	0.80	1.24
y (mm)	0	0.33	0.66	-1.13	0.13	0.85
z (mm)	71	71.36	70.35	70.63	70.35	71.44

4.2.2. Inertia Measurement

Mass properties including center of gravity positions, moment and product of inertias are calculated using the method in Chapter 3.2.3. Equations (3.15) through (3.19) are utilized to obtain the inertia values about point Q. Then, inertia values are also calculated about the center of gravity position using equation (3.20). Similar to the center of gravity measurement in Chapter 4.2.1, the test is run for 60 seconds and equation system in equation (3.15) are constructed.

In Table 6, real and measured values of the mass properties about point Q are given.

Table 6. Complete mass properties measurements about point Q for dummy mass A

	Reference value	Measured value	% Error	Standard Deviation
x (mm)	0	0.78	-	0.44
y (mm)	0	0.97	-	0.99
z (mm)	71	71.38	0.54	0.96
I_x ($kg \cdot m^2$)	0.0606	0.0603	0.50	0.003
I_y ($kg \cdot m^2$)	0.0539	0.0540	0.27	0.001
I_z ($kg \cdot m^2$)	0.0331	0.0328	1.03	0.001
I_{xy} ($kg \cdot m^2$)	0.0057	0.0056	0.67	0.001
I_{xz} ($kg \cdot m^2$)	0	0.0037	-	0.001
I_{yz} ($kg \cdot m^2$)	0	0.0009	-	0.002

As in the center of gravity measurement, the results given in Table 6 are calculated using 8000 Hz data sampling rate. Five different tests are performed with that frequency and the average of the measurements and standard deviations are given in the table. For different data sampling rates, measurements for mass properties are given in Table 7.

Table 7. Measurement of mass properties for different data sampling rates for dummy mass A

	Reference	Measured values				
	Value	100 Hz	500 Hz	1000 Hz	4000 Hz	8000 Hz
$x \ (mm)$	0	0,62	1.02	2.06	0.48	0.78
$y \ (mm)$	0	0,65	0.80	-0.73	0.31	0.97
$z \ (mm)$	71	71,32	70.34	70.68	70.33	71.38
$I_x \ (kg \cdot m^2)$	0.0606	0,0618	0.0613	0.0617	0.0602	0.0603
$I_y \ (kg \cdot m^2)$	0.0539	0,0554	0.0551	0.0534	0.0530	0.0540
$I_z \ (kg \cdot m^2)$	0.0331	0,0327	0.0326	0.0304	0.0322	0.0328
$I_{xy} \ (kg \cdot m^2)$	0.0057	0,0054	0.0058	0.0047	0.0053	0.0056
$I_{xz} \ (kg \cdot m^2)$	0	0,0037	0.0040	0.0067	0.0035	0.0037
$I_{yz} \ (kg \cdot m^2)$	0	0,0002	0.0007	-0.0024	-0.0007	0.0009

Inertia measurements given in Table 6 and Table 7 are about point Q. Inertia measurement about center of gravity are calculated using parallel axis theorem and shown in Table 8. The results in Table 8 are also for 8000 Hz data sampling rate.

Table 8. Inertia measurements about center of gravity for dummy mass A

	Reference value	Measured value	% Error	Standard Deviation
$I_{x,G}$ $(kg \cdot m^2)$	0.0253	0.0231	8.91	0.002
$I_{y,G}$ $(kg \cdot m^2)$	0.0186	0.0168	9.69	0.001
$I_{z,G}$ $(kg \cdot m^2)$	0.0324	0.0327	0.96	0.001
$I_{xy,G}$ $(kg \cdot m^2)$	0.0057	0.0056	0.73	0.001
$I_{xz,G}$ $(kg \cdot m^2)$	0	0.0033	-	0.001
$I_{yz,G}$ $(kg \cdot m^2)$	0	0.0004	-	0.002

If the results are examined, the following implications can be made.

- Results for the center of gravity measurements are pretty accurate. The errors in center of gravity measurements are in a range of ±1 mm

- About point Q, moment of inertia measurements are accurate within ±1% limit.

- Errors are increased when inertia measurements are made about center of gravity. About center of gravity, moment of inertia measurements are accurate within ±10%.

- Also, errors in measurement for product of inertias are in the range of ±0.003 kg·m² for both about point Q and center of gravity position.

4.3. CASE III – DUMMY MASS – B

In this case, a dummy mass consisting of two aluminum block with known dimensions and densities is examined. They are connected to each other at specified points. Their reference mass properties are directly taken from the CAD model to compare the measured values also in this case. Configuration of the test setup is shown in Figure 39.
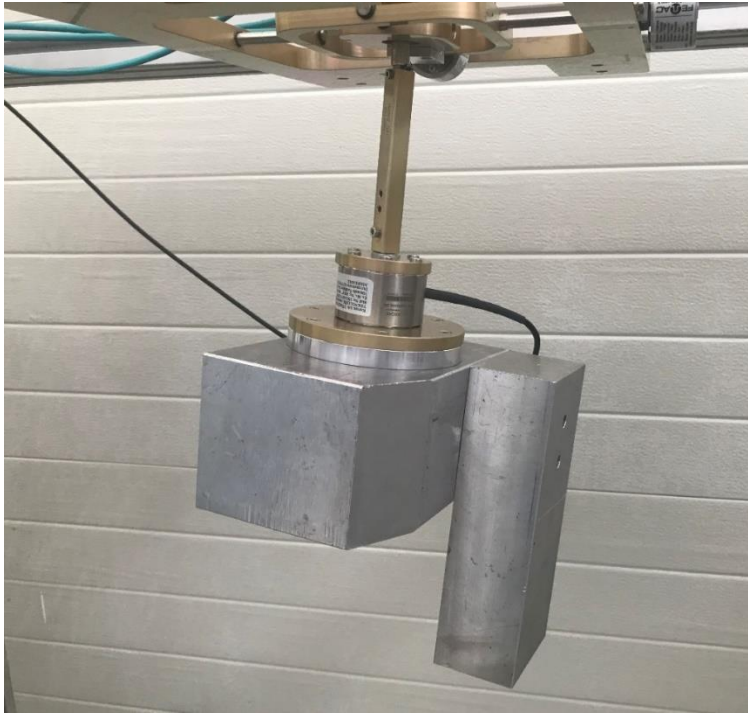
Figure 39. Mass properties of the shown dummy mass consists of two aluminum
block are measured.

The mass of the dummy mass (10.5 kg) is measured in advance and replaced into
equations. The other mass properties are measured with the test device. Similar
procedure as in the Case II is applied to measure mass properties.

4.3.1. Center of Gravity Measurement

In order to measure center of gravity position, similar procedure in Chapter 4.2.1 is
applied. In Table 9, real and measured values of center of gravity position with respect
to point Q are given.

Table 9. Center of gravity position measurements for dummy mass B

	Reference value	Measured value	% Error	Standard Deviation
x (mm)	18.26	19.07	4.46	1.24
y (mm)	-29.46	-30.30	2.84	2.20
z (mm)	91.39	91.38	0.01	1.62

The results given in Table 9 are calculated using 8000 Hz data sampling rate. 5 different tests are performed with that frequency and the average of the measurements and standard deviations are given in the table. Similar to Case II, different data sampling rates are also used. For comparison, center of gravity measurements for different data sampling rates are given in Table 10.

Table 10. Center of gravity position measurements for different sampling rates for dummy mass B

	Reference	Measured values				
	Value	100 Hz	500 Hz	1000 Hz	4000 Hz	8000 Hz
$x \, (mm)$	18.26	20.22	20.18	18.88	18.77	19.07
$y \, (mm)$	-29.46	-29.76	-30.63	-30.29	-28.87	-30.30
$z \, (mm)$	91.39	91.51	91.41	91.01	90.73	91.38

4.3.2. Inertia Measurement

In order to make inertia measurement, similar procedure in Chapter 4.2.2 is applied. In Table 11, real and measured values of the mass properties about point Q are given.

Table 11. Complete mass properties measurements about point Q for dummy mass B

	Reference value	Measured value	% Error	Standard Deviation
$x \, (mm)$	18.26	17.92	1.84	0.668
$y \, (mm)$	-29.46	-29.30	0.53	1.774
$z \, (mm)$	90.39	91.11	0.79	1.617
$I_x \, (kg \cdot m^2)$	0.1585	0.1580	0.30	0.003
$I_y \, (kg \cdot m^2)$	0.1341	0.1360	1.47	0.002
$I_z \, (kg \cdot m^2)$	0.0740	0.0772	4.29	0.003
$I_{xy} \, (kg \cdot m^2)$	-0.0113	-0.0108	4.34	0.001
$I_{xz} \, (kg \cdot m^2)$	0.0244	0.0280	14.77	0.002
$I_{yz} \, (kg \cdot m^2)$	-0.0394	-0.0430	9.21	0.004

As in the center of gravity measurement, the results given in Table 11 are calculated using 8000 Hz data sampling rate. Five different tests are performed with that frequency and the average of the measurements and standard deviations are given in the table. For different data sampling rates, measurements for mass properties are given in Table 12.

Table 12. Measurement of mass properties for different data sampling rates for dummy mass B

	Reference Value	Measured values				
		100 Hz	**500 Hz**	**1000 Hz**	**4000 Hz**	**8000 Hz**
$x \, (mm)$	18.26	19.07	18.20	17.69	17.88	17.92
$y \, (mm)$	-29.46	-29.02	-29.16	-29.05	-28.29	-29.30
$z \, (mm)$	90.39	91.42	91.14	90.83	90.54	91.11
$I_x \, (kg \cdot m^2)$	0.1585	0.1648	0.1620	0.1594	0.1576	0.1580
$I_y \, (kg \cdot m^2)$	0.1341	0.1436	0.1392	0.1386	0.1356	0.1360
$I_z \, (kg \cdot m^2)$	0.0740	0.0798	0.0835	0.0779	0.0774	0.0772
$I_{xy} \, (kg \cdot m^2)$	-0.0113	-0.0104	-0.0102	-0.0111	-0.0099	-0.0108
$I_{xz} \, (kg \cdot m^2)$	0.0244	0.0361	0.0286	0.0301	0.0294	0.0280
$I_{yz} \, (kg \cdot m^2)$	-0.0394	-0.0467	-0.0445	-0.0442	-0.0404	-0.0430

Inertia measurements given in Table 11 and Table 12 are about point Q. Inertia measurement about center of gravity are calculated using parallel axis theorem and shown in Table 13. The results in Table 13 are also for 8000 Hz data sampling rate.

Table 13. Inertia measurements about center of gravity for dummy mass B

	Reference value	Measured value	% Error	Standard Deviation
$I_{x,G}$ $(kg \cdot m^2)$	0.0676	0.0627	7.32	0.006
$I_{y,G}$ $(kg \cdot m^2)$	0.0486	0.0463	4.66	0.004
$I_{z,G}$ $(kg \cdot m^2)$	0.0620	0.0649	4.74	0.003
$I_{xy,G}$ $(kg \cdot m^2)$	-0.0059	-0.0053	9.26	0.001
$I_{xz,G}$ $(kg \cdot m^2)$	0.0078	0.0111	41.08	0.002
$I_{yz,G}$ $(kg \cdot m^2)$	-0.0127	-0.0153	20.67	0.003

If the results are examined, the following implications can be made.

- Results for the center of gravity measurements are more accurate than the results of inertia measurements.
- Accuracy of the center of gravity measurements are better when complete mass properties are calculated simultaneously (4.2.2), rather than measuring only the center of gravity positions (4.2.1). The errors are lower than 4% when only the center of gravity are measured while the errors are lower than 2% when complete mass properties are measured.
- About point Q, moment of inertia measurements are accurate within 5% whereas product of inertia measurements are accurate within 15%.
- Errors are increased when the inertia values are measured about center of gravity position. About center of gravity, moment of inertia measurements are accurate within 10% whereas product of inertia measurements are accurate within 40%.

4.5.   RESULTS AND DISCUSSION

Computer simulation case is the ideal case, in which there is no errors in angle, force or load measurements. Therefore, the theory of the design is checked with a computer simulation first. In that case, accuracy of the measurements is quite high. Error percentages are higher in product of inertia measurements than the other measurements. The reason is that the product of inertia values are smaller compared to other mass properties.

Also, two different real tests are performed. In Case II, mass properties of the dummy mass A are measured. In that case, center of gravity location is on the z axis, which makes the loading symmetric. However, in Case III, the loading is asymmetric since the center of gravity position is not along z axis. Due to the symmetry, the motion of the mass is smoother in Case II. Therefore, errors in the measurements are lower in that case. These errors mostly caused by the geometric imperfectness. Also, the measurement sensibility of the sensors is another error source. The accuracy of the developed design for symmetric (Case II) and asymmetric (Case III) loading are shown in Table 14 and Table 15.

Table 14. Accuracies of the device about point Q

Mass property	Accuracy in Symmetric Loading	Accuracy in Asymmetric Loading
Center of gravity positions (x, y, z)	1 %	2 %
Moment of inertia (I_{xx}, I_{yy}, I_{zz})	1 %	5 %
Product of inertia (I_{xy}, I_{xz}, I_{yz})	1 %	15 %

Table 15. Accuracies of the device about center of gravity

Mass property	Accuracy in Symmetric Loading	Accuracy in Asymmetric Loading
Center of gravity positions (x, y, z)	1 %	2 %
Moment of inertia (I_{xx}, I_{yy}, I_{zz})	10 %	10 %
Product of inertia (I_{xy}, I_{xz}, I_{yz})	1 %	40 %

In Table 14 and Table 15, for symmetric loadings, center of gravity position at x and y axes are zero. Also, product of inertia values, I_{xz}, I_{yz}, are zero. Therefore, these values are ignored in percentage accuracy calculation in Table 14 and Table 15.

While translating inertia values from point Q to center of gravity point, center of gravity measurements are used by taking their squares in parallel axis theorem in equation (2.51). These center of gravity measurements also include errors. Therefore, accuracies for inertia measurements get worse when calculated about center of gravity position instead of point Q as seen in Table 14 and Table 15.

Generally, geometric tolerances of parts of the device are loose and there are unignorable clearances in the assembly. Therefore, some discontinuities occur during the motion of the test specimen. That makes the measurements of the rotation angles different from the actual values.

Also, it is assumed that all the coordinate axes perfectly coincide at a specific point; however, there are some offsets in the axes due to the loose tolerances in the assembly. Therefore, reference point, point O or point Q, can be different from the ideal position. Since the inertia values are proportional to the square of the displacements, these offsets highly effect the accuracy of the inertia measurements.

The reference values of the measured object are taken from CAD software, since the measured object are simple; however, these values cannot be measured exactly with

a software due to the nonhomogeneity of the objects. Therefore, reference values, which are used to compare the measured values, also includes some errors.

The encoders are incremental type encoders and they should be brought into the reference position each time they start. Thus, in the starting of each test, the virtual coordinate system attached to the test specimen is aligned with the fixed reference coordinate system to make the angle measurements starting from zero. For that purpose, a water gauge is used to level the specimen in x and y axes. The alignment in z axis is ensured by visually only. Therefore, in each test, there is $\pm 0.5°$ error in angle measurements.

There is one differentiation operation in the velocity calculations and two differentiation operations in the acceleration calculations. These differentiation operations are made using discrete angular position measurements. If a small error occurs in the angle measurement of the encoder, there may be some jumps in the derivative of these measurements. That causes the mismeasurement of the velocities and accelerations of the test specimen.

During the tests, data are collected with two different data acquisition systems, one for encoders and one for load sensor. The data acquisition device for the load sensor has eight channels and six of them are used for force and torque measurements. Since, three more channels are required for the angle measurements, a separate data acquisition device is used for encoders. Therefore, these data acquisition systems cannot be started at the same time exactly. Some time differences, which are about 0.1 second, occurs between load and angle measurements.

Also, there are some errors in the measurements of the encoders and load sensor due to their sensitivities. That creates errors in the calculation of mass properties.

CHAPTER 5

CONCLUSION AND FUTURE WORK

Measuring the mass properties is an important task to design a moving system. This thesis includes the design of a device that can measure mass properties of an object with a mass up to 20 kg. The main objective of the design is to measure all the mass properties in a single test configuration. Some concepts in the literature, used for that purpose, are explained in the thesis. In the developed design, favorable aspects of these concepts are utilized to make the design simple and accurate.

The developed device directly uses the Newton's equation of motion to determine mass properties of the test specimen. Making oscillatory rotational motion of the test specimen without using actuators is the main simplicity of the design. Eliminating the need of an actuator makes the design cost-effective, also.

Three different cases are studied to check over the convenience of the design. One of these cases is a computer simulation using MSC Adams software. In that simulation, all the inputs, which are used to calculate mass properties, can be exactly measured using the software. Using these measurements in the calculation procedure gives the mass properties accurate in a range of $\pm0.5\%$, which shows the feasibility of the developed design for measuring the mass properties of an object in a single test configuration.

In the other cases, two different dummy masses are used to measure mass properties. The errors are changing with the symmetry of loading. When the loading is symmetric, the measurements are more accurate.

In future study, there are going to be some improvements for the developed test device and a new device are going to be produced. In the manufactured device, geometric tolerances are loose and it causes offsets and large clearances in the assembly. Since these offsets and clearances are not included in calculations, the accuracy of the results are effected. Therefore, in the next manufacturing process, the tolerances are going to be kept tight and the errors due to geometric tolerances are going to be lowered.

Further, the velocities and accelerations, which are used in measurement process of the current design, are obtained by differentiating the angular position measurements. One differentiation operation is made to get velocities and two differentiation process to get accelerations are made. Inherently, differentiation operation is not sensitive when limited discrete data points are used. For this reason, in the following design, accelerometers are going to be used to measure velocities and accelerations. Acceleration values are going to be directly taken from the accelerometers and velocities are going to be calculated by integrating the accelerometer measurements.

In addition, in the developed design, data are collected separately for encoders and load sensor due to the capability of the data acquisition systems. Between these two data acquisition systems, there are ~0.1 s difference. In the next design, a data acquisition system with more channels, at least nine channels, are going to be used to eliminate synchronization shift in the current design.

The developed design can measure masses up to 20 kg due to the capacity of the load sensor. With the mentioned improvements, a new device is going to be produced for masses lower than 20 kg. Then, increasing the size and the load sensor capacity, one more device is going to be produced for masses up to 1000 kg.

REFERENCES

[1]   R. C. Hibbeler, *Statics and Dynamics*, no. January. 2002.

[2]   G. W. Housner and D. E. Hudson, "Applied Mechanics Dynamics," *Div. Eng. - Calif. Inst. Technol.*, p. 399, 1980.

[3]   K. Özgören, *Robot Manipülatörlerin Dinamiği ve Kontrolü.* .

[4]   J. Gingsberg, *Engineering Dynamics*. 2010.

[5]   R. Boucher, D. Rich, H. Crane, and C. Matheny, "A Method for Measuring the Product of Inertia and the Inclination of the Principal Longitudinal Axis of Inertia of an Airplane," 1954.

[6]   P. Micelles, "US Army Test And Evaluation Command Test Operatıons Procedure - Center Of Gravity," *Polymer (Guildf).*, pp. 9–16, 2005.

[7]   P. Hejtmanek, O. Blatak, and J. Vancura, "New approach to measure the vehicle center of gravity height," *Perner's Contacts*, vol. X, no. 4, pp. 18–27, 2015.

[8]   A. Shakoori, A. V. Betin, and D. A. Betin, "Comparison of three methods to determine the inertial properties of free-flying dynamically similar models," *J. Eng. Sci. Technol.*, vol. 11, no. 10, pp. 1360–1372, 2016.

[9]   R. S. Boynton and K. Wiener, "A new high accuracy instrument for measuring moment of inertia and center of gravity," *SAWE Tech. Pap. n.1827*, no. 1827, pp. 1–17, 1988.

[10]   P. E. Uys, P. S. Els, M. J. Thoresson, K. G. Voigt, and W. C. Combrinck, "Experimental Determination of Moments of Inertia for an Off-Road Vehicle in a Regular Engineering Laboratory," *Int. J. Mech. Eng. Educ.*, vol. 34, no. 4, pp. 291–314, 2006.

[11]   R. Boynton, "3238. Measuring weight and all three axes of center of gravity of a rocket motor without having to reposition the motor," *61st Annu. Conf. Virginia Beach, Virginia, May 18-22*, no. 3238, p. 22, 2002.

[12]   R. Boynton and K. Wiener, "Measuring Mass Properties of Aircraft Control Surfaces," no. 3020, 2014.

[13]   L. Klaus, T. Bruns, and M. Kobusch, "Moment of Inertia and Damping of Components of the Dynamic Torque Calibration Device," 2012.

[14]   A. Kotikalpudi, B. Taylor, C. Moreno, H. Pfifer, and G. J. Balas, "Swing Tests for Estimation of Moments of Inertia," pp. 1–7.

[15]   C. B. Winkler, "Inertial Properties of Commercial Vehicles, Descriptive Parameters Used in Analyzing the Braking and Handling of Heavy Trucks," vol. 2, no. April, 1983.

[16]   M. Cooper and P. Titchener, "Trifilar Pendulum : Measurement and Error Analysis," vol. 2013, pp. 1–30, 2013.

[17]   P. Y. Chai, "Moment of Inertia Measurement for Propulsion System," no. 1, pp. 3–5, 2007.

[18]   A. J. Swank, C. Hardham, K. Sun, and D. B. Debra, "Five-Wire Torsion Pendulum and Optical Sensing."

[19]   J. L. du Bois, N. A. J. Lieven, and S. Adhikari, "Error Analysis in Trifilar Inertia Measurements," *Exp. Mech.*, vol. 49, no. 4, pp. 533–540, 2009.

[20]   B. Wang, Z. X. Hou, X. Z. Gao, and S. Q. Shan, "The Application Of Inertial Measurement Unit in Inertia Parameter Identification," vol. 201–203, pp. 974–981, 2011.

[21]   R. A. Mattey, "Bifilar Pendulum."

[22]   A. L. Korr and P. Hyer, "A Trifilar Pendulum for the Determination of Moments of Inertia," pp. 1–6, 1962.

[23]   L. Tang and W. Bin Shangguan, "An Improved Pendulum Method For The Determination Of The Center Of Gravity And Inertia Tensor For Irregular-Shaped Bodies," *Meas. J. Int. Meas. Confed.*, vol. 44, no. 10, pp. 1849–1859, 2011.

[24]   Z. C. Hou, Y. ning Lu, Y. xin Lao, and D. Liu, "A new trifilar pendulum approach to identify all inertia parameters of a rigid body or assembly," *Mech. Mach. Theory*, vol. 44, no. 6, pp. 1270–1280, 2009.

[25]   M. R. Eicholtz, J. J. Caspall, P. V Dao, S. Sprigle, and A. Ferri, "Test Method For Empirically Determining İnertial Properties Of Manual Wheelchairs," vol. 49, no. 1, pp. 51–62, 2012.

[26]   C. S. Barnes and A. A. Woodfield, "Measurement of the Moments and Product of Inertia of the Fairey Delta 2 Aircraft," *Aeronaut. Res. Counc. Reports Memo.*, no. 3620, 1970.

[27]   P. W. Poels, "Cogging Torque Measurement , Moment of Inertia Determination and Sensitivity Analysis of an Axial Flux Permanent Magnet AC motor," p. 54, 2008.

[28]   D. H. Perry, "Measurements of the Moments of Inertia of the Avro 707B Aircraft," *Minist. Aviat. Aeronaut. Res. Counc. Curr. Pap.*, 1961.

[29]   P. Hejtmánek, O. Blaťák, P. Kučera, P. Porteš, and J. A. N. Vančura, "Measuring the Yaw Moment of Inertia of a Vehicle," *J. Middle Eur. Constr. Des. Cars*, pp. 16–22, 2013.

[30]   Y. Yang and B. Wang, "Methods to Measure the Rotational Inertia of Rocket Projectiles of Ultra Large Diameter," no. Icadme, pp. 2165–2168, 2015.

[31]   P. L. Ringegni, M. D. Actis, and A. J. Patanella, "Experimental Technique For Determining Mass Inertial Properties Of Irregular Shape Bodies And Mechanical Assemblies," *Meas. J. Int. Meas. Confed.*, vol. 29, no. 1, pp. 63–75, 2001.

[32]   M. Gobbi, G. Mastinu, and G. Previati, "A method for measuring the inertia properties of rigid bodies," *Mech. Syst. Signal Process.*, vol. 25, no. 1, pp. 305–318, 2011.

[33]   M. Gobbi, G. Mastinu, M. Pennati, and G. Previati, "InTenso+ System: Measured Centre of Gravity Locations and Inertia Tensors of Road Vehicles," *Vol. 3 16th Int. Conf. Adv. Veh. Technol. 11th Int. Conf. Des. Educ. 7th Front. Biomed. Devices*, vol. 3, p. V003T01A037, 2014.

[34]   M. Bacaro, F. Cianetti, and A. Alvino, "Device for measuring the inertia properties of space payloads," *Mech. Mach. Theory*, vol. 74, pp. 134–153, 2014.

[35]   R. Brancati, R. Russo, and S. Savino, "Method and equipment for inertia parameter identification," *Mech. Syst. Signal Process.*, vol. 24, no. 1, pp. 29–40, 2010.

[36] H. Hahn, K. D. Leimbach, and A. Piepenbrink, "Inertia parameter identification of rigid bodies using a multi-axis test facility," *Proc. Third IEEE Conf. Control Appl.*, vol. \bf 3, pp. 1735–1737, 1994.

[37] J. A. Mangus, C. Passerello, and C. Vattkarsen, "Estimating Rigid Body Properties from Force Reaction Measurements," pp. 469–472.

[38] V. G. Melnikov, "A new method for inertia tensor and center of gravity identification," *Nonlinear Anal. Theory, Methods Appl.*, vol. 63, no. 5–7, pp. 1377–1382, 2005.

[39] T. Tian, H. Jiang, Z. Tong, J. He, and Q. Huang, "An inertial parameter identification method of eliminating system damping effect for a six-degree-of-freedom parallel manipulator," *Chinese J. Aeronaut.*, vol. 28, no. 2, pp. 582–592, 2015.

[40] O. Tuncer and S. Ç. Başlamışlı, "a Procedure for the Online Measurement of a Vehicle'S Inertia Tensor on a Stewart Platform," 2008.

[41] R. A. B. Almeida, A. P. V. Urgueira, and N. M. M. Maia, "Identification of rigid body properties from vibration measurements," *J. Sound Vib.*, vol. 299, no. 4–5, pp. 884–899, 2007.

[42] R. A. B. Almeida, A. P. V. Urgueira, and N. M. M. Maia, "Evaluation of the Performance of Three Different Methods Used in the Identification of Rigid Body Properties," *Shock Vib.*, vol. 15, no. 3–4, pp. 467–479, 2008.

[43] R. A. B. Almeida, A. P. V. Urgueira, and N. M. M. Maia, "Further developments on the estimation of rigid body properties from experimental data," *Mech. Syst. Signal Process.*, vol. 24, no. 5, pp. 1391–1408, 2010.

[44] A. W. Chin, C. Y. Herrera, N. D. Spivey, W. A. Fladung, and D. Cloutier, "Testing and validation of the dynamic inertia measurement method," *Conf. Proc. Soc. Exp. Mech. Ser.*, vol. 9, pp. 81–104, 2015.

[45] A. Fareed and F. Wahl, "Identification of rigid body parameters using experimental modal analysis data," *Technische Mechanik*, vol. 21, no. 3. pp. 63–75, 2001.

[46] A. Fregolent and A. Sestieri, "Identification of Rigid Body Inertia Properties From Experimental Data," *Mech. Syst. Signal Process.*, vol. 10, no. 6, pp. 9–13, 1996.

[47] R. De Gray, "Experimental Identification of the Characteristics of an Rigid Structure on an Elastic Suspension," pp. 955–961.

[48] S. J. Huang and G. Lallement, "Direct estimation of rigid body properties from harmonic forced responses," *Proc. Int. Modal Anal. Conf. - IMAC*, vol. 1, pp. 175–180, 1997.

[49] R. Kloepper, H. Akita, M. Okuma, and S. Terada, "An Experimental Identification Method for Rigid Body Properties Enabled by Gravity-Dependent Suspension Modelling," *1st Jt. Int. …*, 2010.

[50] R. Kloepper and M. Okuma, "Experimental identification of rigid body inertia properties using single-rotor unbalance excitation," *Proc. Inst. Mech. Eng. Part K J. Multi-body Dyn.*, vol. 223, no. 4, pp. 293–308, 2009.

[51] D. R. Lazor Jr., "Considerations For Using The Dynamic Inertia Method In Estimating Rigid Body Inertia Property," *Couns. Educ. Superv.*, 2008.

[52] H. Lee, Y.-B. Lee, and Y.-S. Park, "Response and Excitation Points Selection for Accurate Rigid-Body Inertia Properties Identification," *Mech. Syst. Signal Process.*, vol. 13, no. 4, pp. 571–592, 1999.

[53] A. Malekjafarian, M. R. Ashory, and M. M. Khatibi, "Identification of inertia properties from the results of output-only modal analysis," *Arch. Appl. Mech.*, vol. 83, no. 6, pp. 923–937, 2013.

[54] A. Malekjafarian, M. R. Ashory, M. M. Khatibi, and M. Saberlatibari, "Rigid body stiffness matrix for identification of inertia properties from output-only data," *Eur. J. Mech. A/Solids*, vol. 59, pp. 85–94, 2016.

[55] A. Malekjafarian, M. R. Ashory, M. M. Khatibi, and M. S. Latibari, "A new method for estimation of rigid body properties from output-only modal data," *4th Int. Oper. Modal Anal. Conf. IOMAC 2011*, pp. 454–461, 2011.

[56] A. Malekjafarian, M. R. Ashory, and M. M. Khatibi, "Estimation of Rigid Body Properties from the Results of Operational Modal Analysis," *Modal Anal.*, no. Mm, 2010.

[57] E. Mucchi, S. Fiorati, R. Di Gregorio, and G. Dalpiaz, "Comparison of Techniques in Time and Frequency Domain," *IMAC-XXVII, Orlando, Florida USA*, no. Mmm, 2009.

[58] S. M. Pandit, Y.-X. Yao, and Z.-Q. Hu, "Dynamic Properties of the Rigid Body and Supports from Vibration Measurements," *J. Vib. Acoust.*, vol. 116, no. 3, pp. 269–274, 1994.

[59] S. M. Pandit and Z.-Q. Hu, "Determination Of Rigid Body Characteristics From Time Domain Modal Test Data," *J. Sound Vib.*, vol. 177, no. 1, pp. 31–41, 1994.

[60] C. Schedlinski and M. Link, "On the identification of rigid body properties of an elastic system," *Proc. Int. Modal Anal. Conf. - IMAC*, vol. 2, pp. 1588–1594, 1997.

[61] C. Schedlinski and M. Link, "Identification of rigid body properties using base excitation and measured interface forces," *Eur. Sp. Agency, (Special Publ. ESA SP*, no. 386 PART 2, pp. 689–697, 1996.

[62] A. P. V Urgueira, "On the Rigid Body Properties Estimation From Modal Testing," *Int. Modal Anal. Conf. (IMAC XIII), Nashville, Tennessee USA*, pp. 1479–1483, 1995.

[63] M. C. Witter, D. L. Brown, and J. R. Blough, "Measuring the Six-DOF Driving Point Impedance Function and an Application to RB Inertia Property Estimation," *Mech. Syst. Signal Process.*, vol. 14, no. 1, pp. 111–124, 2000.

[64] E. Mucchi, G. Bottoni, and R. Di Gregorio, "Determining the rigid-body inertia properties of a knee prosthesis by FRF measurements," 2009.

[65] J. Toivola and O. Nuutila, "Comparison of three methods for determining rigid body inertia properties from frequency response functions," *Proc. SPIE - Int. Soc. Opt. Eng.*, p. 1126, 1993.

[66] C. Schedlinski and M. Link, "A survey of current inertia parameter identification methods," *Mech Syst Signal Pr*, vol. 15, no. 1, pp. 189–211, 2001.

[67] L. Meirovitch, "Fundamentals of Vibrations," *Applied Mechanics Reviews*, vol. 54, no. 6. p. B100, 2001.

[68] B. N. Taylor and A. Thompson, "The International System of Units," *Nist Spec. Publ. 330 2008 Ed.*, p. 92, 2008.

[69] E. Ientilucci, "Using the singular value decomposition," *Rochester Inst. Technol.*, pp. 1–8, 2003.

[70] F. Cheli and G. Diana, *Advanced dynamics of mechanical systems*. 2015.

[71] D. T. Greenwood, *Advanced Dynamics*. 2003.

APPENDIX A

SPECIFICATIONS OF ROTARY ENCODERS

Specifications of the rotary encoders used in measurement process are given.

|		
Resolution (steps/turn)	:	2048 pulse/revolution
Voltage Supply	:	4.75 VDC to 30 VDC
Consumption w/o Load	:	$\leq$ 60 mA (24 VDC)
Output Frequency	:	> 200 kHz
Output Signal	:	90° shifted A and B, Z+ inverted
Shaft Loading	:	$\leq$ 60 N axial, $\leq$ 80 N radial
Operating Speed	:	$\leq$ 10000 rpm
Starting Torque	:	$\leq$ 0.020 Nm
Weight	:	150 g
Part Number	:	FNC 40H 8630V-2048-R2

Figure A-1. Outlook of the rotary encoder
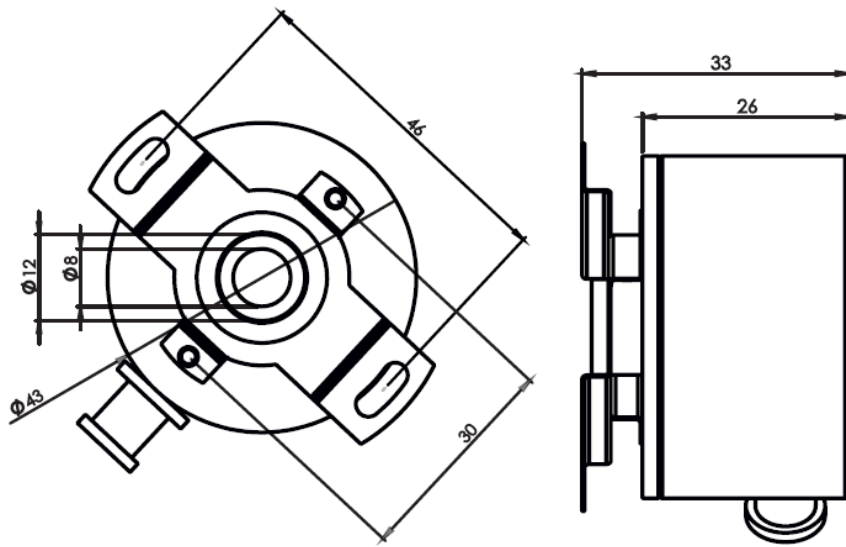
Figure A-2. Dimensions of the rotary encoder

APPENDIX B

SPECIFICATIONS OF LOAD SENSOR AND AMPLIFIER

Technical specifications of six-axis load sensor and amplifier are given.

Nominal Force, F_x	:	200 N
Nominal Force, F_y	:	200 N
Nominal Force, F_z	:	500 N
Nominal Torque, M_x	:	5 Nm
Nominal Torque, M_y	:	5 Nm
Nominal Torque, M_z	:	10 Nm
Rated Output	:	0.4 mV/V
Zero Signal	:	< 2 mV/V
Excitation Voltage of Load Sensor	:	5 V
Rel. Linearity Deviation	:	0.1 %
Rel. Zero Signal Hysteresis	:	0.1 %
Rel. Repeatability Error	:	0.5 %
Part Number of Load Sensor	:	K6D40-200N/5Nm/CG
Input Voltage of Amplifier	:	± 10 V
Number of Analogue Inputs	:	8
Input Sensitivities	:	7 mV/V, 3.5 mV/V, 2 mV/V
Analog output of Amplifier	:	± 10 V
Number of Analogue Outputs	:	8
Supply Voltage of Amplifier	:	12-28 V
Part Number of Amplifier	:	GSV-8DS SubD44HD

Figure B-1. Outlook of the load sensor
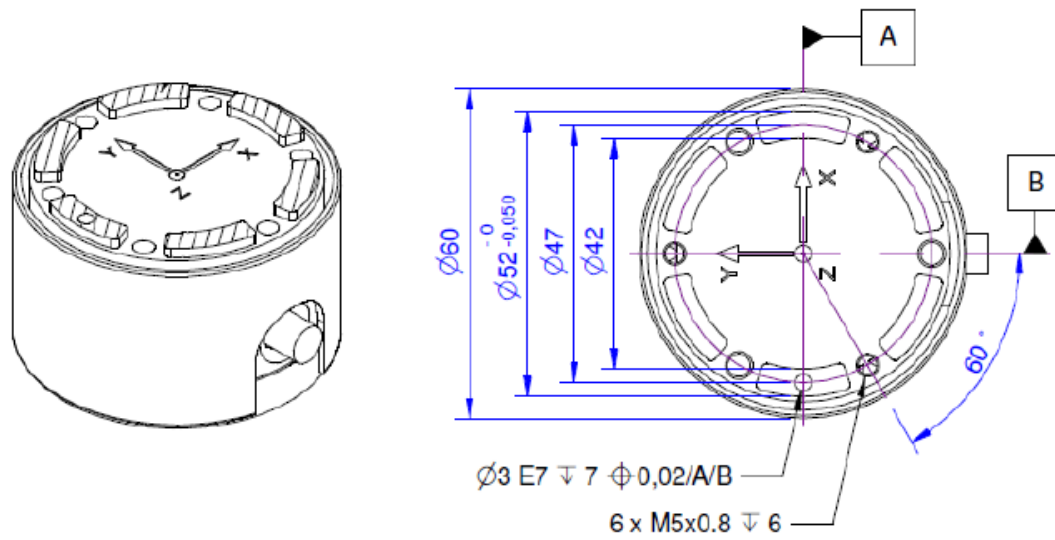
**Figure B-2.** Dimensions of the load sensor

Figure B-3. Front and back sides of the amplifier

EULER'S ANGLES, EULER'S ROTATION SEQUENCE AND ANGULAR VELOCITY ABOUT BODY FIXED COORDINATE SYSTEM

Chapter 3.1 of [71] is utilized here to explain the Euler's angles, Euler's rotation sequence and the procedure to obtain angular velocities using Euler's angle.

A rigid body can be repositioned in any orientation by composing three rotations about coordinate axes. Euler angles are defined by three of these rotations. These rotations can be done in any sequence. For instance, 123 rotation sequence incidates that the rotations are applied about x, y and z axis, respectively.

In the rotation sequence, one axis can be repeated, e.g., 313, 121, 232, 323, 131, 212 sequences. The angles for these rotations are called Proper Euler angles. If there is no repeated axis in the sequence, e.g., 123, 231, 312, 132, 321, 213 sequences, their rotation angles are called Bryan or Cardan angles.

For each rotation, a transformation matrix is formed using direction cosines. The rotation sequence applied to the test configuration is 123 sequence in which the first rotation is θ_1 about x axis, the second rotation is θ_2 about y axis and the third rotation is θ_3 about z axis. Transformation matrices for these rotations are formed as follows

$$T_x = \begin{bmatrix} 1 & 0 & 0 \\ 0 & \cos\theta_1 & \sin\theta_1 \\ 0 & -\sin\theta_1 & \cos\theta_1 \end{bmatrix},$$

$$T_y = \begin{bmatrix} \cos\theta_2 & 0 & -\sin\theta_2 \\ 0 & 1 & 0 \\ \sin\theta_2 & 0 & \cos\theta_2 \end{bmatrix}, \tag{C.1}$$

$$T_z = \begin{bmatrix} \cos\theta_3 & \sin\theta_3 & 0 \\ -\sin\theta_3 & \cos\theta_3 & 0 \\ 0 & 0 & 1 \end{bmatrix}.$$

Transformation matrix which converts the first coordinate system to the final coordinate system are constituted as follows

$$T = T_z\, T_y\, T_x,$$

$$T = \begin{bmatrix} \cos\theta_3 & \sin\theta_3 & 0 \\ -\sin\theta_3 & \cos\theta_3 & 0 \\ 0 & 0 & 1 \end{bmatrix} \begin{bmatrix} \cos\theta_2 & 0 & -\sin\theta_2 \\ 0 & 1 & 0 \\ \sin\theta_2 & 0 & \cos\theta_2 \end{bmatrix} \begin{bmatrix} 1 & 0 & 0 \\ 0 & \cos\theta_1 & \sin\theta_1 \\ 0 & -\sin\theta_1 & \cos\theta_1 \end{bmatrix},$$

$$T = \begin{bmatrix} \cos\theta_2\cos\theta_3 & \cos\theta_1\sin\theta_3 + \sin\theta_1\sin\theta_2\cos\theta_3 & \sin\theta_1\sin\theta_3 - \cos\theta_1\sin\theta_2\cos\theta_3 \\ -\cos\theta_2\sin\theta_3 & \cos\theta_1\cos\theta_3 - \sin\theta_1\sin\theta_2\sin\theta_3 & \sin\theta_1\cos\theta_3 + \cos\theta_1\sin\theta_2\sin\theta_3 \\ \sin\theta_2 & -\sin\theta_1\cos\theta_2 & \cos\theta_1\cos\theta_2 \end{bmatrix}$$

$$\tag{C.2}$$

Derivative of the Euler's angles does not directly the angular velocities of a body, they should be converted into the body frame. 123 rotation sequence is demonstrated in the Figure 45.
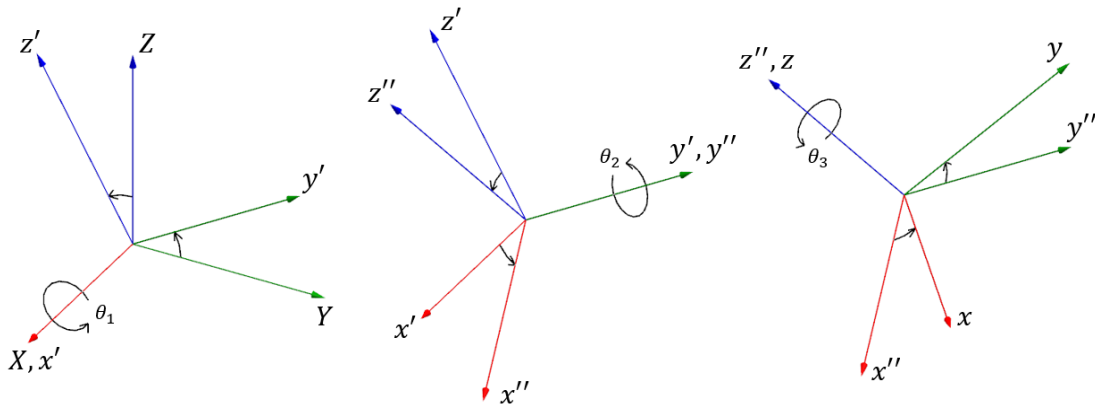

Figure C-1. Euler angles in 123 rotation sequence

According to the figure, the first rotation (θ_1) is measured in the reference coordinate system (XYZ). Therefore, it should be transformed into the body-fixed coordinate system (xyz) by applying transformation matrices about x axis first, then about y axis and lastly about z axis with the following transformation matrix

$$T_{123} = T_z T_y T_x. \tag{C.3}$$

Similarly, the second rotation (θ_2) is measured in the first intermediate coordinate system ($x'y'z'$). It should be transformed into the body-fixed coordinate system with the following transformation matrix

$$T_{23} = T_z T_y. \tag{C.4}$$

Lastly, the third rotation (θ_3) is measured in the second intermediate coordinate system ($x''y''z''$). It should be transformed into the body-fixed coordinate system with the following transformation matrix

$$T_3 = T_z. \tag{C.5}$$

Afterwards, in order to find the angular acceleration of the body in the body-fixed coordinate system, transformations given in equations (C.1) should be applied to the derivative of the rotation measurements in the following way

$$\omega = T_{123} \begin{Bmatrix} \dot{\theta}_1 \\ 0 \\ 0 \end{Bmatrix} + T_{23} \begin{Bmatrix} 0 \\ \dot{\theta}_2 \\ 0 \end{Bmatrix} + T_3 \begin{Bmatrix} 0 \\ 0 \\ \dot{\theta}_3 \end{Bmatrix}. \tag{C.6}$$

If transformation matrices are replaced into equation (C.6) and required operations are made, the following relation for the angular velocities about body-fixed coordinate system is obtained for 123 rotation sequence

$$\omega = \begin{Bmatrix} \omega_x \\ \omega_y \\ \omega_z \end{Bmatrix} = \begin{bmatrix} \cos\theta_1\cos\theta_3 & \sin\theta_3 & 0 \\ -\cos\theta_1\sin\theta_3 & \cos\theta_3 & 0 \\ \sin\theta_1 & 0 & 1 \end{bmatrix} \begin{Bmatrix} \dot{\theta}_1 \\ \dot{\theta}_2 \\ \dot{\theta}_3 \end{Bmatrix}. \tag{C.7}$$

Then, angular accelerations can be directly calculated by taking the derivatives of the angular velocities as follows

$$\alpha = \dot{\omega}. \tag{C.8}$$